Techno-economic evaluation of the potential of CO_2 storage and Enhanced Oil Recovery in the Niger-Delta Hydrocarbon Basin using reservoir simulation: Case Study.

Precious Ogbeiwi [1,*] , Karl D Stephen [1]

[1] Institute of GeoEnergy Engineering, Heriot-Watt University, Edinburgh, EH14 4AS, UK.

[*] Corresponding Author

This manuscript has been submitted for publication in **Journal of Petroleum Exploration and Technology**. Please note that the manuscript is undergoing peer review and is yet to be formally accepted for publication. Subsequent versions of this manuscript may have slightly different content. Please feel free to contact the corresponding author; we welcome feedback

Abstract:

The constant dependence on fossil fuel combustion for energy and industrial activities results in global warming and climate change due to the increased atmospheric concentration of greenhouse gases such as CO_2. CO_2 storage in mature petroleum reservoirs is considered one of the most viable ways to reduce CO_2 concentrations in the atmosphere. The Niger-Delta hydrocarbon basin holds significant volumes of petroleum and is, therefore, a prime candidate for CO_2 storage. This study uses a case study of a mature oil reservoir to assess the techno-economic potential for CO_2-enhanced oil recovery and storage in the Niger Delta. The methodology used a suitable screening criterion to assess the feasibility of the case study reservoir for CO_2 EOR and storage. The reservoir's carbon storage and incremental oil recovery potentials were then estimated. A new economic model for the CO_2 storage project in the Niger-Delta petroleum basin was developed and applied to establish the commercial viability of the CO_2 flooding project. Sensitivity and uncertainty analyses were then performed to assess the economic risks associated with the project. Our results showed that the properties of the reservoir make it suitable for miscible CO_2 injection and that the reservoir has huge potential for enhancing oil production by CO_2 injection while storing a vast amount of the injected carbon in the subsurface. The economic study and uncertainty analysis results also revealed that CO_2-enhanced oil recovery and storage in the Niger-Delta basin is economically viable even under economic uncertainties, and a relatively low oil price.

1. INTRODUCTION

Human activities such as the combustion of fossil fuels and biomass, bushfires, and various manufacturing and mining processes all contribute to higher CO_2 and other greenhouse gas (GHG) concentrations. According to the International Energy Agency (IEA), CO_2 emissions from the combustion of fossil fuels are the most significant source of rising CO_2 concentrations in the atmosphere, accounting for approximately 75% of current global emissions (IEAGHG, 2009). The most substantial emissions come from power plants and high-energy-consuming industries, and mechanisms such as carbon capture and sequestration (CCS) are now in place to ensure that these sectors drastically reduce emissions. (Aminu, Nabavi, Rochelle, & Manovic, 2017).

CCS is a set of procedures that begin with capturing CO_2 from high-carbon-emitting industrial and utility plants such as oil and gas facilities, power plants, cement factories, and so on, transporting it to subsurface storage via trucking for small volumes or piping networks for larger volumes, and then permanently storing it in a secure reservoir using a variety of options. According to the International Energy Agency's 2008 Energy Technology Perspective Report, CCS could eliminate nearly 20% of global CO_2 emissions by 2050 (IEAGHG, 2009). Because of various variables, including economic considerations, accessibility of the storage site, and secure storage of the injected gas in the subsurface, underground CO_2 storage in geological formations has been recognised as the best sequestration option. Furthermore, the existence of highly permeable rock and an impermeable layer of capping seals in these storage limits the possibility of CO_2 leakage from the reservoir (Safi, Agarwal, & Banerjee, 2016). As a result, subsurface geological storages provide long-term subsurface CO_2 storehouse, lowering GHG emissions in the atmosphere, particularly when sequestration is carried out on a big scale. Sequestration in geological formations, according to Leung et al., (2014), can reduce emissions from power plants by 80-90% when fully implemented.

Because of its various advantages, CO_2 storage in matured or depleted petroleum reservoirs, such as those explored in this work, is one of the viable geological storage choices. Firstly, substantial studies on depleted and mature petroleum reservoirs have been undertaken prior to and during petroleum resource development and production, thus their storage capacity is rather well known. There are also surface and subsurface facilities, including as injectors and pipeline networks, that can be utilised for CO_2 storage with or without minor modifications (Bachu et al., 2004). Finally, mature petroleum reservoirs are thought to be favourable for CO_2 storage and increased oil recovery due to an excellent geologic seal or caprock that has contained hydrocarbons for an extended period of time. Furthermore, the geological features of these reservoirs are rather well understood, lowering the amount of related uncertainties and dangers, especially when compared to alternative kinds of underground CO_2 storage (Stewart, Johnson, Heinemann, Wilkinson, & Haszeldine, 2018).

CO_2 storage in depleted oil and gas or other geo-energy reservoirs also improves the energy resource recovery potential, making them more economically viable (Aminu et al., 2017; Leung et al., 2014). Because the global average recovery factor in a typical petroleum reservoir is approximately 35-40%, enhanced hydrocarbon recovery techniques in mature or depleted reservoirs using CO_2 as the injection fluid are widely used globally to improve

recovery (Stalkup, 1978; Zahoor et al., 2011; Aminu et al., 2017). The increased revenue generated by this incremental production could help offset the additional expenditures associated with CO_2 injection (Godec et al., 2013; Solomon, 2006). Carbon capture, utilisation, and storage (CCUS) activities utilise captured CO_2 as an injection fluid for better petroleum resources or geothermal system recovery for higher energy production (Safi et al., 2016).

This study investigates the potential of West Africa's offshore Niger-Delta hydrocarbon region for CCUS, i.e., long-term secured CO_2 storage and enhanced oil recovery. To do so, we used a suitable screening criterion to assess the suitability of a mature turbidite petroleum reservoir in the Niger Delta hydrocarbon province for CO_2 enhanced oil recovery and sequestration, determining the minimum miscibility pressure, and evaluating the storage and hydrocarbon production capacities. The theoretical and effective storage capacity of the case study reservoir was evaluated using well-established methodologies, available data, and full-physics numerical simulations of the case study reservoir. Because the economic feasibility of a project has a greater influence on decision-making than its technical feasibility, a novel economic model for the CO_2 Enhanced Oil Recovery (EOR) process in the Niger-Delta case study was then presented in order to estimate the Net Present Value (NPV) of the region's CO_2 EOR and storage processes. The NPV, the objective function, and a methodology that included sensitivity analysis, experimental design for uncertainty sampling, and uncertainty analysis using Monte Carlo simulation were then used to examine the economics and commercial risk of the CO_2 flooding project.

2. BACKGROUND

2.1. Screening of Reservoirs for CO_2 storage. To assess the viability of a reservoir candidate for CO_2 storage, acceptable screening criteria are applied (Raza et al., 2016). Relevant studies has been conducted to define appropriate screening criteria for CO_2 sequestration in aquifers, geothermal, and petroleum (oil and gas) resources (Chadwick et al., 2008; Kovscek, 2002; Ramírez, Hagedoorn, Kramers, Wildenborg, & Hendriks, 2010; Raza et al., 2016; Solomon, 2006). Kovscek, (2002) devised a screening criterion for depleted oil reserves for CO_2 sequestration. Formation thickness, depth, storage capacity, fluid volumes in place, and permeability were all considered. CO_2 density was identified as an important component for the site selection procedure in his work. The relationship between hydrocarbon production and faults and fracture reactivations was also highlighted. Solomon (2006) established a selection criterion for an EOR technique that takes into account

parameters such as injection depth, CO_2 and brine density, reservoir properties, the presence of contaminants, and storage durations. Chadwick et al., (2008) evaluated a localised-scale criterion based on results and observations from five European CO_2 injection operations in their analysis.. Ramírez et al., (2010) used a Multi-Criteria Analysis (MCA) technique to develop a screening criterion for rating the viability and storage capacity of reservoirs in the Netherlands, such as aquifers, gas, and oil reservoirs, for long-term carbon sequestration. They identified storage capacity, prices, and reservoir sites as crucial screening parameters. Raza et al., (2016) developed a more robust screening criterion for mature hydrocarbon gas reserves using the factors described by Chadwick et al., (2008) and additional significant factors in their research. Table 1 outlines some of the screening criteria reported in previous research and by other authors.

To consider miscible CO_2 EOR flood in a reservoir, the reservoir pressure, Pi, must be at least 200 psi higher than the measured minimum miscibility pressure (MMP) of the reservoir oil, and the Pi/MMP ratio must be greater than or equal to 1 (Bachu, 2003). Furthermore, faults can only be categorised as seals if they have a permeability of less than 0.1 mD and are surrounded by impermeable rocks such as clay and evaporites (Van Der Meer, 2005).

Table 1. A summary of screening criteria for CO_2 storage sites.

Pressure	Reservoir type studied	CO_2 Storage Capacity	Seal properties	Seal composition	Reservoir Pressure, psia	Reservoir Composition	Oil Saturation	Φ (%)	K (mD)	K_v/k_h	Crude oil density	Pay thickness	Depth of injection	Oil Viscosity (mPa.s)	Oil Gravity (^{0}API)	Res. Temp.
Carcoana, (1982)	Miscible Oil				> 8.3 MPa (1200 psia)		> 30%		> 1		< 0.8227		< 3000m (9800ft)	< 2	> 40	< 90^{0}C (195^{0}F)
Taber, (1983)	Oil						> 30%				< 0.8948		> 700m	< 15	> 26	
Klins, (1984)					> 10.3 MPa		>25%				< 0.8762		> 914m	< 12	> 30	
Zhao, (2001)	Oil						> 20%				< 0.9218		< 762m	< 10	> 22	
Bachu et al., (2004)	Oil				> 7.6 MPa		> 25%				0.8924 – 0.7883				27 - 48	32 – 120^{0}C
Solomon, (2006)	Oil				10 – 15 MPa > MMP					Low K_v (< 0.5)		Thin reservoir (< 20m)	> 600m		> 27 (Light oils)	
Chadwick et al., (2008)	Oil	> the total CO_2 production from the source.	Caprock must not have faults and a thickness between 20 - 100m	Must be salt, anhydrite, shale or claystone				> 20	> 300		30 – 100 g/L	>> 20m	1000 – 2500m			
Raza et al., (2016)	Depleted Gas reservoir	Total estimated capacity > amount of CO_2 produced from source.	Caprock must not have faults and be between 20 – 100m thick					10 – 20	10 – 100		Low	20 - 50m	800 – 2000m			
Ramírez et al., (2010)	Aquifer and oil reservoir	≥ 4 Mt for Aquifer and ≥ 10 Mt for petroleum reservoirs	No faults with thickness ≥ 10m	Salt, anhydrite, shale or claystone		Aquifer: Limestone, Petroleum systems: limestone, sandstones, siltstone, carbonate		> 10	>= 200			> 10m	≥ 800m			

2.2. Reservoir Properties of the Storage Site. The Niger-Delta Basin is located in the Gulf of Guinea, West Africa, and stretches throughout the Niger-Delta hydrocarbon region. Since the Eocene period, it has advanced southwestward, resulting in a series of depo-belts that are its most active region at each stage of formation and form one of the world's largest regressive deltas with an area of approximately 300,000 km^2 (Doust H. & Omatsola E. M., 1990, Kulke, 1995 as cited by Oyeyemi et al., 2018). The average thickness of the sediment at the middle of the depo-belt is around 10 km, with an estimated volume of 500,000 km^3 (Kaplan et al., (1994) as cited by Tuttle et al., (1999)). The interested reader is referred to studies by Doust H. & Omatsola E. M., (1990); Kehinde & Ahzegbobor, (2015); Liu et al., (2013a); Ofurhie, Lufadeju, Agha, & Ineh, (2008); Opara, (2011); Stacher, (1995); Tuttle et al., (1999) for a better understanding of Niger Delta geology.

In summary, the Niger-Delta hydrocarbon province is made up of a regressive clastic sequence with a maximum thickness of approximately 9,000-12,000 m (29,500-39,400 ft.) and a surface area of nearly 75,000 km2, making it suitable for CO_2 storage (Doust H. & Omatsola E. M., 1990; Umar, Gholami, Nayak, Shah, & Adamu, 2020). The basin's faulting intensity is moderate, and its hydrogeology is distinguished by an excellent regional flow system (Umar et al., 2020). The basin is considered a mature hydrocarbon province due to its significant exploration and production history. The basin is divided into three distinct formations that characterise its depositional facies and are classified based on their shale volumes: the Akata, Agbada, and Benin Formations. Relevant investigations by other authors (Luna, 2013; Tuttle et al., 1999; Liu et al., 2013; Namdie et al., 2017; Opara, 2011; Oyeyemi et al., 2018; Umar et al., 2020). provide further information concerning these formations. Figure 1 depicts a dip section of the Niger Delta, highlighting three unique formations.

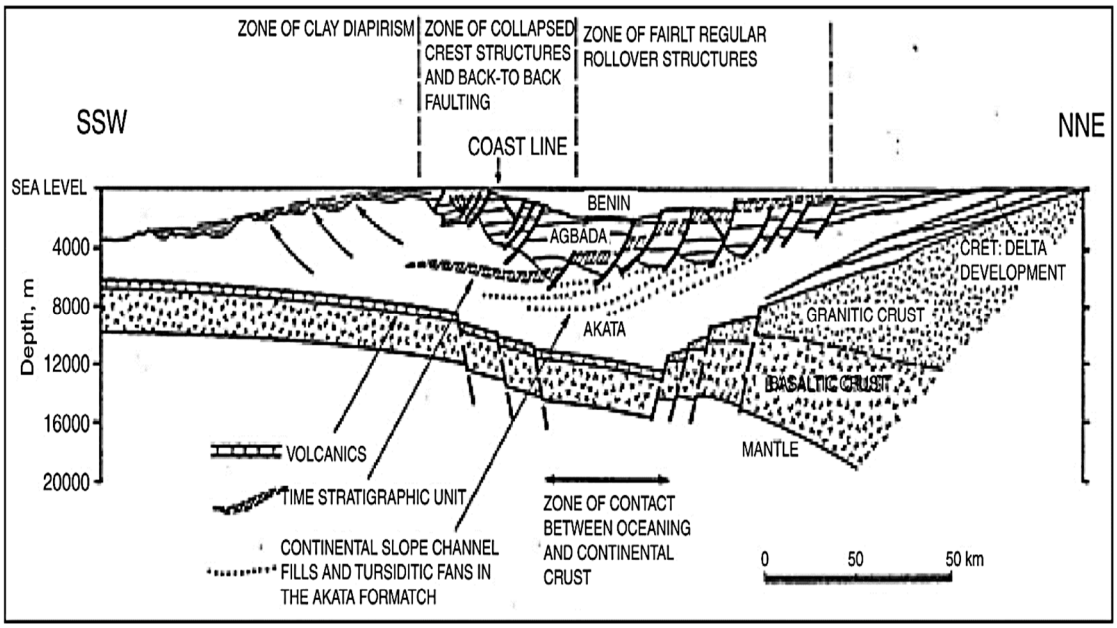

Figure 1. Schematic of the Niger Delta dip section (Modified from Weber and Daukoru, 1975 as cited by Adegoke et al., 2017)

The Niger-Delta hydrocarbon basin has the most natural gas reserves in Africa, and its hydrocarbon exploration and production (E&P) activities have continuously released enormous amounts of carbon into the atmosphere, primarily due to flaring of unwanted produced gas (Oni & Oyewo, 2011). The Nigerian National Petroleum Corporation (NNPC statistical bulletins 1997 - 2011) (see Appendix) contains the distribution of gas sources in the Niger Delta, as well as a statistical analysis of the volumes of gas produced and the percentage of flared gas from hydrocarbon reservoirs in the basin (Umar et al., 2020). Figure 2 depicts the table graphically as well as a map of the Niger-Delta with treservoir locations and volumes of gas produced and flared. In some offshore areas, up to 100% of the produced gas is flared. It depicts the hydrocarbon province's abundance of gas flares, which can be utilised as potential source points. The CO_2 produced by flaring activities can be captured and securely stored in the subsurface utilising known carbon capture technology. For example, captured gas can be used to boost oil and gas recovery by using CO_2 EOR to maintain reservoir pressure and increase oil and gas production, or it can be injected and securely stored in subsurface rocks for future use.

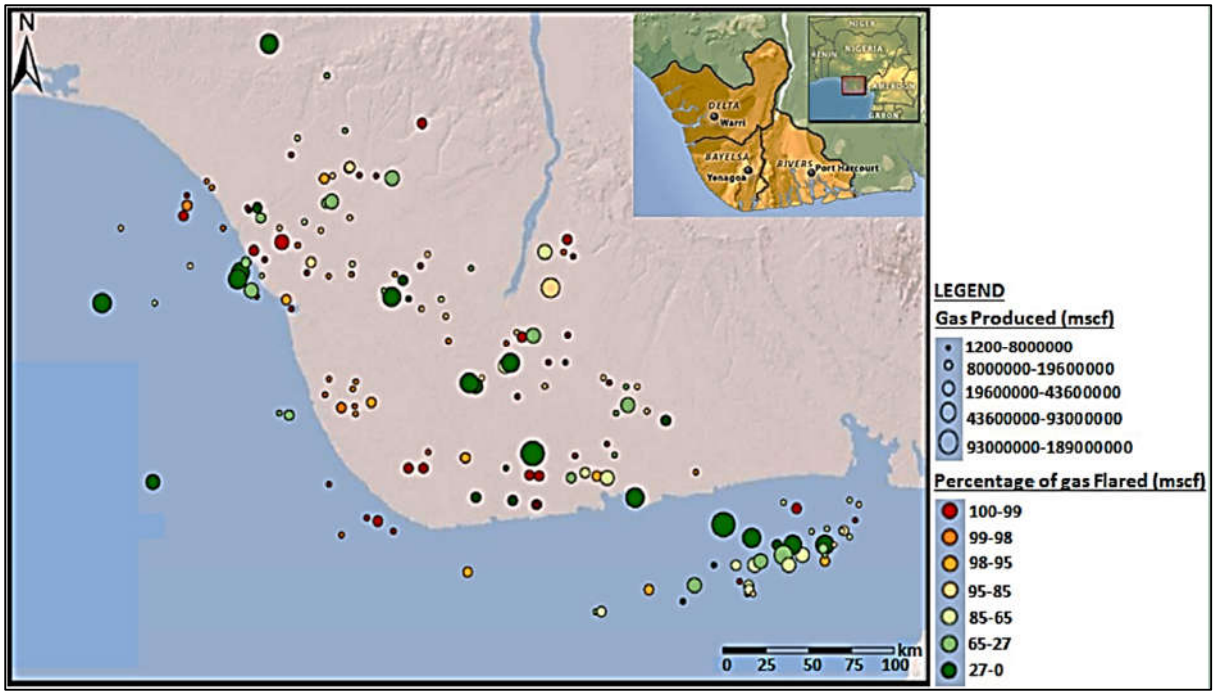

Figure 2. Map of the Niger Delta showing gas sources, the amount of gas produced and flared from hydrocarbon reservoirs in the basin (from Umar et al., 2020)

To reduce gas flaring, the Federal Government of Nigeria and the oil firms operating in the area established certain approaches to gas utilisation programmes (Umar et al., 2020). These options include gas-to-power (GTP) plants and gas gathering projects that were implemented to support the government's efforts to provide gas for export to the worldwide market. Other techniques include using the gas as a raw material in petrochemical facilities, re-injection for hydrocarbon reservoir management, and using the gas as fuel in local manufacturing units. Carbon emissions from these gas usage schemes are also significant CO_2 sources for CCUS in the Niger-Delta region. Cement manufacture, fertiliser production, and other chemical businesses in various regions of the basin are also point sources of pollution (i.e., CO_2 emissions in the basin).

Carbon emissions from gas flaring owing to hydrocarbon E&P activities were considered the principal source of CO_2 for CCS efforts in the basin in this paper based on these discussions and studies conducted by Oni and Oyewo, (2011) and Umar et al., (2020). The flared carbon was anticipated to be captured using well-established carbon capture technologies such as post-combustion, pre-combustion, and oxyfuel combustion methods and then injected into the subsurface formation for secure storage and EOR (Leung et al., 2014; Rhodes, 2013).

2.3. Case Study: Field Description and the Reservoir Simulation Model. The case study reservoir is a 4450-foot-deep undersaturated oil reservoir in the offshore Niger Delta. The primary drive during the early stages of reservoir drainage was provided by reservoir fluid expansion. However, as drainage progressed, the massive support supplied by the underlying aquifer provided the energy required for production (Arinkoola, Onuh, & Ogbe, 2016). Due to hydraulic faulting, the porous medium is divided into four zones with absolute permeabilities ranging from 100 to 1300 mD (a mean of 500 mD) and porosities ranging from 10 to 27% (an average of 13.94%) (Precious Ogbeiwi, Stephen, & Arinkoola, 2020). Arinkoola et al., (2016) provides a full summary of the case study reservoir parameters to interested readers.

Arinkoola et al., (2016) demonstrated the case study's original geostatic model and primary production method. Ogbeiwi et al., (2020) described the secondary (waterflood) production approach. Figure 3 depicts the position of the wells on a map showing the reservoir's porosity. The numerical simulation model was constructed on a grid of 100 × 100 x 25 cells representing the x, y, and z directions.

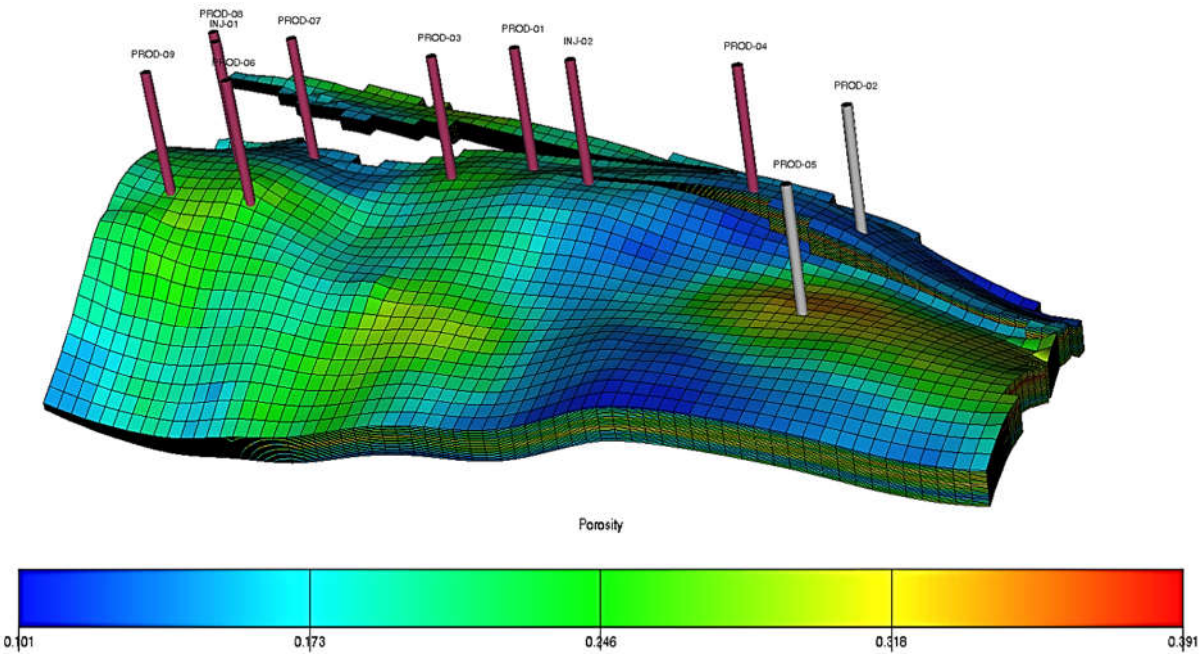

Figure 3. Top-surface reservoir model with porosity distribution and well placement.

Each cell measured an average of 300 × 300 x 1ft and was constructed using corner-point geometry. The fluid contacts, namely gas-oil and oil-water, were located at 4444 and 4585 feet, respectively, and the numerical simulations were carried out using the Schlumberger E300 compositional reservoir simulator. The model's properties are summarised in Table 2.

Table 2. Average properties of the case study reservoir model

Property	***Value***
Porosity, $\varnothing$	13.94%
Saturation of water at oil-water contact, S_w	27%
Sandstone net-to-gross, NTG	87%
Permeability, k	500mD
Reservoir thickness,	250ft
Initial reservoir pressure, P_i	1950psia
Initial reservoir temperature, T_i	110^0F
Oil viscosity, μ_o	0.31cP
Water viscosity, μ_w	0.395cP
Oil density, ρ_o	57.98 lb/ft^3 (0.929 t/m^3)
Water density, ρ_w	62.43 lb/ft^3
Reference reservoir depth	4450ft
Oil initial formation volume factor, (FVF)	1.22 RB/STB
Anisotropy (k_V/k_H)	0.6

Due to the absence of relative permeability functions for the case study reservoir, the measurements from an analogous reservoir were modified through a history-matching routine and applied to the Niger-Delta turbidite reservoir (Arinkoola & Ogbe, 2015). Two-phase relative permeability curves were presented, and the Stone II model was used to compute the three-phase curves. Figure 4 depicts the relative permeability curves for the oil-water and gas-oil systems for the various reservoir areas studied in this study.

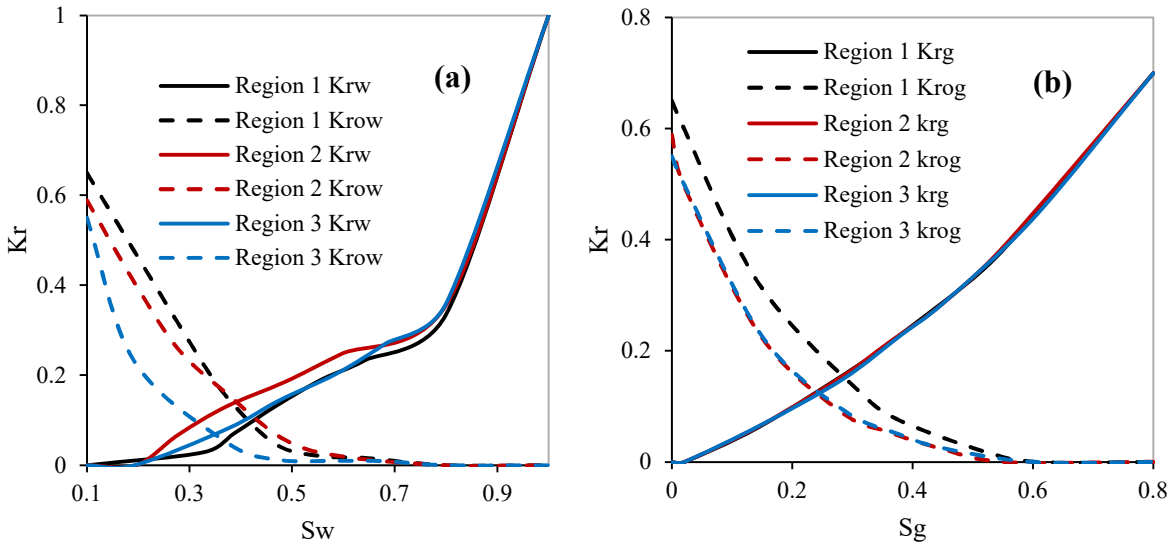

Figure 4. Relative permeability functions for the (a) oil-water and (b) gas-oil systems

2.4. The compositional fluid model. Complex flow interactions with phase behaviour are captured and modelled by compositional fluid models (Li & Durlofsky, 2016). Since they can predict the reservoir's phase behaviour and displacement behaviour, the actual compositions of hydrocarbon phases due to their complicated PVT behaviour are explicitly accounted for. Compositional simulations can model miscible floods (Al-Mudhafar et al., 2018a; Esmaiel et al., 2007; Naderi and Simjoo, 2019; Vahidi et al., 2014). The Schlumberger ECLIPSE PVTi software was used to create a compositional model for the numerical modelling of reservoir fluid flow and phase behaviour during the CO_2 enhanced oil recovery in this investigation. Using a modified Peng-Robinson Equation of State (EOS), the compositional model was divided into seven components. Table 3 shows the PVT parameters employed in this investigation, while Table 4 shows the initial oil composition.

Table 3. EOS parameters for the different components of the fluid model.

Component Names	CO_2	C1	C_2-nC_4	iC_5-C_6	HYP01	HYP02	HYP03
Molecular Weights (g/mol)	44.01	16.04	38.4	72.82	135.82	257.75	330.998
Omega A	0.46	0.46	0.46	0.46	0.46	0.46	0.46
Omega B	0.08	0.08	0.08	0.08	0.08	0.08	0.08
Critical T (K)	376.244	215.626	353.668	469.3	621.341	779.695	847.748
Critical P (bar)	47.73	81.303	51.576	35.747	25.142	13.861	10.318
Acentric Factors	0.142	0.47	0.136	0.224	0.438	0.837	1.056
Volume Shift	-0.083	0.074	-0.086	-0.043	0.022	0.226	0.334
Component Parachors	153.228	74.912	137.52	233.896	393.596	662.45	843.128
Mol Fraction, frac.	0.0095	0.1904	0.1142	0.1428	0.2761	0.1428	0.1242

Table 4. *Composition of the initial oil*

Component	CO_2	C_1	$C_2 – nC_4$	$iC_5 – C_6$	HYP1	HYP2	HYP3
Initial oil (%)	1.18	11.7	19.5	22	28.2	9.4	8.1

2.5. Calculating the Minimum Miscibility Pressure. The pressure threshold at which the flood changes from immiscible to miscible displacement is defined as the minimum miscibility pressure (MMP) (Kamari, Arabloo, Shokrollahi, Gharagheizi, & Mohammadi, 2015). This quantity, which determines the pressure at which the reservoir's oil and gas acquire multi-contact miscibility, is an important parameter to consider when designing CO_2 injection projects (Kamari et al., 2015; Martin & Taber, 1992). The efficiency of the oil displacement by gas in a miscible flood is a function of reservoir pressure, and the displacement process is only miscible when the pressure is at or above the MMP. The reservoir should be operated at or above the MMP to develop multi-contact miscibility in order to maximise hydrocarbon recovery during a miscible flood (Aghdam, Moghaddas, Moradi, Dabiri, & Hassanzadeh, 2013; Lashkarbolooki, Eftekhari, Najimi, & Ayatollahi, 2017; Vahidi et al., 2014). As a result, inaccurate MMP calculations are detrimental, and it is vital to precisely predict the MMP of CO_2 in oil in order to model reservoir performance during CO_2 injection. To forecast the minimal miscibility pressure of CO_2 in oil, two methods are used: (1) laboratory methods, most notably the slim tube experiment; and (2) empirical, analytical, and numerical methods.

The MMP of CO_2 in oil was determined using a 1-D numerical compositional model of the slim tube experiment and a typical sample of crude oil from the Niger Delta basin acquired from Ghomian, (2008). The numerical simulation experiment used the Peng-Robinson EOS compositional model. According to Vulin et al., (2018)), the slim-tube simulation model included 500 × 1 x 1 cells with diameters of 0.1 x 0.1 x 0.1m. The injection and production wells were located on the model's opposite sides using the petrophysical characteristics and relative permeability functions described in the previous section. CO_2 injection was performed at a reservoir fluid volume target rate of 0.12 rm^3/day in order to achieve a constant injection rate of 2.4 PV/day, and the production well was initially operated at a target bottom-hole pressure (BHP) of 50 bars. The producer's BHP was modified to compute the minimum miscibility pressure of the in-situ oil with the injected gas.

The oil's MMP in CO_2 was calculated to be 80 bars (Figure 5). The Schlumberger PVTi software (2019) produced a value of 80.7 bars (about 1170.46 psia) using the Glasø

correlation (Glasø, 1985 as cited by Ahmadi et al., 2017). This number was similar to the slim-tube experiment simulation results.

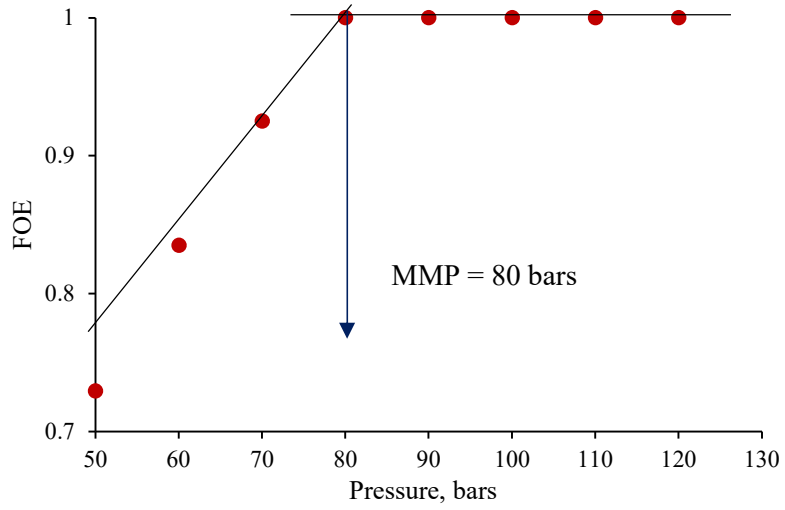

Figure 5. MMP prediction using the slim-tube experiment simulation.

2.6. Hysteresis Effects and Residual Trapping of the Injected CO_2. During CO_2 flooding, the imbibition and drainage gas relative permeability curves undergo cyclic changes (Larsen & Skauge, 1995). This phenomenon known as hysteresis is due to the trapping of the non-wetting phase (i.e., the injected gas) during the imbibition (the water injection) phase, where some of the gas phase gets disconnected from the remaining gas in the form of a blob and becomes trapped and immobile (Spiteri & Juanes, 2006; Assef et al., 2019). This phenomenon is critical to CO_2 flooding because it allows for the trapping of the non-wetting phase and hence the retention and storage of the injected CO_2 in the subsurface (Arogundade et al., 2013; Shahverdi and Sohrabi, 2015; Al-Muftah et al., 2019). Water injectivity is also affected by the saturation of the trapped non-wetting phase. Therefore, to achieve accurate results in the modelling of CO_2 flooding, a reliable hysteresis model must be used.

The trapped gas saturation, denoted as S_{gt} is the most significant factor that characterises the impact of hysteresis during the modelling of CO_2 flooding (Spiteri et al., 2005). Most hysteretic relative permeability models are based on Land's trapping model (Land, 1968). The trapped gas saturation is calculated using this model as follows:

$$S_{gt} = S_{gc} + \frac{S_{g,hy} - S_{gc}}{1 + C(S_{g,hy} - S_{gc})} \quad (1)$$

where S_{gc} is the critical gas saturation, $S_{g,hy}$ is the gas saturation at flow reversal, and C is the Land's trapping parameter, which is calculated from the bounding drainage and imbibition curves as:

$$C = \frac{1}{S_{gt,max} - S_{gc}} - \frac{1}{S_{g,max} - S_{gc}} \quad (2)$$

where $S_{g,max}$ is the maximum gas saturation, and $S_{gt,max}$ is the maximum trapped non-wetting phase saturation, which is described by the imbibition bounding curve. The value of C depends on the rock and fluid properties.

Killough's hysteresis model which considers hysteresis to be a function of Land's trapping parameter was used in this work. This model allows the drainage and imbibition cycles to be reversed along the same scanning curve. The gas phase's relative permeability along the scanning curve is computed as follows:

$$k_{rg}^{i}(S_g) = \frac{k_{rg(o)}^{i}(S_{g,norm}).k_{rg(o)}^{d}(S_{g,hy})}{k_{rg(o)}^{d}(S_{g,max})} \quad (3)$$

where

$$S_{g,norm} = S_{gt,max} + \frac{(S_g - S_{gt})(S_{g,max} - S_{gt,max})}{S_{g,hy} - S_{gc}} \quad (4)$$

In Eq. (3), $k_{rg(o)}^{i}$ and $k_{rg(o)}^{d}$ are the values of the relative values on the bounding imbibition and drainage curves, respectively. Figure 6 depicts the gas relative permeability predicted by Killough's model.

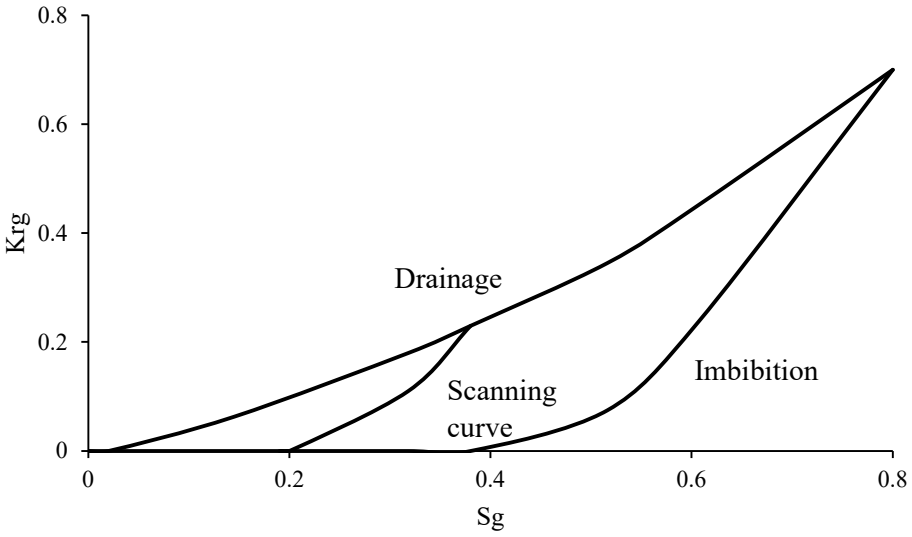

Figure 6. The two-phase gas relative permeability scanning curves

3. ESTIMATING THE ENHANCED OIL RECOVERY AND CO_2 STORAGE CAPACITY DURING CO_2 EOR

3.1. Analytical Prediction. In this study, the potential for enhanced oil recovery and CO_2 storage was calculated using an analytical equation and a numerical simulation model. The methodology used to estimate CO_2 storage capacity was prospect-level assessment. The reservoir fluid storage capacity was assessed using a fluid replacement approach (Bachu et al., 2007; IEAGHG, 2009). As a result, the theoretical and effective storage capacity, which describe the physical and technical limits of the capacity estimate, was calculated as the mass of CO_2 that can be injected into pore spaces previously containing recovered hydrocarbon reserves and any produced water at surface conditions.

These storage capacity estimates were based on some assumptions. First, water from the underlying aquifer was seen during hydrocarbon production, as determined by Arinkoola et al., (2016) 's production, pressure, and saturation history-matching approach. This effect will be discussed more in the next section. Furthermore, despite the fact that the fluid volume data derived from the numerical simulation represents the technically available pore space for carbon storage, the efficiencies of the carbon storage and incremental oil recovery processes were set at 75% to present a more realistic technical limit of the capacities estimate. According to Bachu et al., (2004), this figure is reasonable in oil reservoirs where the density gradient between CO_2 and oil is lower than in CO_2-water systems and when CO_2 is injected under miscible reservoir conditions. The effective storage capacity is represented by the capacities calculated after using this efficiency factor.

The following section describes the calculations for the theoretical carbon storage and enhanced oil recovery potentials. When CO_2 is continually injected into the subsurface, the analytical estimate of the reservoir's carbon storage capacity was reported as (Gozalpour et al., 2005; Bachu et al., 2007):

$$SC_{CO_2} = (RF.V_{oil(stp)} - V_{iw} + V_{pw} + V_{pg})\rho_{CO_2} \quad (5)$$

The enhanced oil recovery by CO_2 injection was estimated as:

$$M_{EOR} = (RF.V_{oil(stp)} \times SW_{CO_2})/\rho_{oil} \quad (6)$$

where $V_{oil(stp)}$= initial oil volume, ρ_{CO_2} = density of CO_2 at reservoir conditions (kg/m^3) and ρ_{oil} = oil density. SW_{CO_2} = sweep efficiency of the flood, V_{iw}, V_{pw} and V_{pg} were volumes of injected or invading water, produced water and gas respectively. The quantity $RF.V_{oil(stp)}$

represented the volume of the recovered oil at surface conditions. Stevens et al., (1999) reported the typical sweep efficiencies of miscible CO_2 floods to be 2.11t/m^3, and this value was applied for the analytical estimation of the incremental oil recovery capacity due to CO_2 injection.

3.2. The Effect of the Underlying Aquifer. Because the reservoir comprises an underground aquifer, the reservoir oil and gas are in hydrodynamic equilibrium with the aquifer water, according to Arinkoola et al., (2016). During primary production, reservoir pressure dropped, and aquifer water invaded the reservoir, lowering the potential net reservoir CO_2 storage capacity. This can also cause reservoir pressure to rise above its initial value during CO_2 injection, albeit this is not always possible due to caprock fracturing and other issues (Bachu et al., 2004). Furthermore, because of hysteresis effects such as changes in irreducible water saturation, displacement of invaded aquifer water may be unachievable, resulting in a permanent loss of storage capacity (Juanes, Spiteri, Orr, & Blunt, 2006; E. J. Spiteri & Juanes, 2006). The history-matching procedure performed by Arinkoola et al., (2016) determined that considerable underlying aquifer support was required to match the reservoir pressure and fluid production history. To account for the effects of the encroaching water influx from the aquifer, we introduced a factor, C_{aq}, into the CO_2 storage capacity formula (Equation 7). This factor represented the reduction in sequestration capacity caused by the underlying aquifer and was given as 0.97 for weak aquifers and 0.50 for oil reservoirs with substantial aquifer support (Bachu et al., 2004; Liang, Shu, Li, Shaoran, & Qing, 2009). According to Liang et al., (2009), this factor can also account for reservoir volume decline due to injected water or aquifer water invasion.

Therefore, the effective storage of CO_2 was estimated using:

$$SC_{CO_2} = (RF.V_{oil(stp)} - V_{iw} + V_{pw} + V_{pg})\rho_{CO_2}.C_{aq}.C_{eff} \quad (7)$$

and the enhanced oil recovery by CO_2 injection was estimated as:

$$M_{EOR} = (RF.V_{oil(stp)} \times SW_{CO_2} \times C_{eff})/\rho_{oil} \quad (8)$$

where C_{eff} is the effective carbon sequestration coefficient which was assumed to be 75%.

3.3. Estimation by Numerical Simulation. The carbon storage capacity estimation equations (Equations 1-4) assumed that the oil reservoir's theoretical CO_2 storage capacity is equal to the pore space previously containing the recovered fluids (oil, gas, and water). As a result, it was necessary to use numerical simulations to validate the analytical estimations of

the sequestration and oil recovery potentials. This is due to the numerical simulations taking into account the effects of water invasion, gravity segregation, viscous fingering, reservoir heterogeneity, relative permeability hysteresis, and other factors that are largely ignored in theoretical estimates (Bachu et al., 2004; Gozalpour et al., 2005). As a result, we calculated the improved oil production and carbon storage potentials using full-physics simulations of a calibrated history-match numerical model of the case study reservoir. Miscible and immiscible CO_2 injection strategies such as continuous gas injection, gravity-stabilizing gas injection, water-alternating gas injection, and other innovative technologies are currently used in CO_2-EOR and storage (Aminu et al., 2017; Gozalpour et al., 2005; Kumar & Mandal, 2017). For clarity, we applied a numerical simulation of miscible continuous CO_2 flooding of the case study reservoir to calculate the reservoir potentials after the field had gone through the primary and secondary production stages (Arinkoola et al., 2016; P Ogbeiwi, Stephen, & Arinkoola, 2020). Existing wells were reworked/recompleted, and water injectors were converted to gas injectors.

The following is the operating strategy for continuous CO_2 injections: For 24 years, continuous CO_2 injection into the reservoir was carried out utilising the existing water injectors. To guarantee that the flooding was miscible, the injector and producer BHPs were kept above the MMP at 3000 and 1170 psia, respectively. Each producer's target production rate was set at 1000 stb/d, while the target gas injection rate was set at 10000 Mscf/day. The economic cut-off for the production wells was set at 50 STB/day, a gas-oil ratio of 10000 Mscf/STB, and a water cut of 95%. After 24 years, the reservoir's enhanced oil recovery potential and carbon storage potential were determined based on the total volume of oil produced and CO_2 retained in the subsurface.

4. ECONOMIC MODEL AND RISK ANALYSIS FOR CO_2 EOR AND SEQUESTRATION PROCESSES IN THE NIGER-DELTA HYDROCARBON BASIN

The commercial viability of a project, which can be represented by an economic model, has a greater influence on the decision-making process than the technical feasibility of the project (Tang et al., 2014; Yang et al., 2007). As a result, the viability of a project must be quantified in terms of its economic value rather than its technical and performance potential. We evaluated the economics and commercial risk of the CO_2 flooding project in this section. The workflow included developing an economic model, screening and sensitivity analysis, experimental design, and uncertainty analysis using Monte Carlo simulation (MCS). The objective function in this case was the net present value (NPV) of the CO_2 injection project,

calculated as the discounted cashflow over the 24-year injection period. This function accounted for capital and operating costs, taxes and royalties, CO_2 transportation and capture costs, as well as appropriate incomes and penalties. The effects of cost and income parameters on the economic objective function were investigated in our study. We used Nigeria's current fiscal laws for oil and gas (ETF, 1993; PPT, 1990; PTDF, 1990). However, in the absence of data and due to the sensitivity studies, reasonable assumptions were made using data from well-established projects in similar provinces such as Brazil, China, Canada, and others (Lawal, 2011; Tang et al., 2014; Wei et al., 2015a; He et al., 2016; Pham and Halland, 2017; Dai et al., 2017).

The net annual cash flow profile had to be determined in order to build an economic model. This was after deducting the yearly cash input and outflow streams, as well as the "allowable" fixed asset depreciation. The annual cash flow was calculated using the following relationship (Shell, 2001):

$$NCF = R_V - C_{CAPEX} - C_{OPEX} - C_{ROY} - C_{TAX} - C_{CO2} \quad (9)$$

where R_V was the total income, C_{CAPEX}, C_{OPEX}, C_{ROY}, and C_{TAX} were the capital expenditure, fixed and variable operating expenditure, royalty, and tax, respectively. C_{CO2} was the monetary fine for any fugitive carbon emissions. The gross revenue R_V was made up of cash inflows from hydrocarbon resource sales and any income earned as a result of carbon storage in the subsurface.

The royalty and tax expenditures, C_{ROY} and C_{TAX} were calculated as:

$$C_{ROY} = r_r R_V', \quad (10)$$

$$C_{TAX} = r_t(R_V - C_{ROY} - C_{OPEX} - C_{DEP}) \quad (11)$$

where r_r and r_t are royalty and tax rates, respectively. C_{DEP} is the fiscal depreciation, and R_V' is the gross revenue less revenues from carbon credits. Every estimate is made on a yearly basis. The royalty and tax disbursements are government receipts as a result of Nigeria's fiscal policies (Lawal, 2011; Echendu and Iledare, 2016). Even though the carbon credit generated revenue, it was taxed separately and was not included in royalty payments. This was due to the fact that, unlike oil and gas sales income, carbon credit revenues were unrelated to the extraction of natural resources. In addition, the expenses of decommissioning were factored into the annual net cash flow estimate in the year of abandonment.

The NPV objective function was computed using the NCF and was given by:

$$NPV = \sum_{i=1}^{n} \frac{NCF}{(1+r_D)^i} \quad (12)$$

where r_D and n_t denoted the discount rate and project duration prior to the year of abandonment, respectively, and i denoted the year counter. The discount rate was used to amortise the capital expenditure over the project's lifecycle (Sun & Chen, 2022). The analyses in this study were conducted during a period of 24 years of CO_2 injection.

The discussion in the following subsections focuses on the critical variables of the NPV objective function. We also discussed the assumptions we used in our computations.

4.1. The Capital Expenditure (CAPEX) and Operating Expenditure (OPEX) Components. The capital cost relates to well, flowlines and processing facilities. Considerations should also be made for gas compression and CO_2 compression facilities. Given the existence of flowing producers, injectors, and existing surface facilities in the reservoir, some of the capital costs in this study were computed based on the need to convert the existing water injection facilities to CO_2 flooding facilities (McCoy & Rubin, 2008). Because the reservoir was a mature oil field, capital expenditures included the cost of drilling and completing additional injectors and producers, as well as the costs of their associated surface facilities. These were necessary to reduce well spacing, improve pattern uniformity, and improve the fluid displacement profiles and economic incentives for the project. In summary, the CAPEX evaluated in the study included workover expenses for current producers and injectors, pattern production and injection equipment, CO_2 processing equipment, and drilling and completion expenditures for new wells. Costs linked with contingencies and decommissioning were also budgeted for.

The project's operation and maintenance costs included regular daily expenses as well as other consumable charges such as gas injection, oil treatment, CH_4 treatment, water handling, and surface and subsurface facility maintenance. Following CO_2 breakthrough at the production wells, any produced CO_2 can be collected and utilised for injection with the purchased CO_2. This signifies that the cumulative volume of CO_2 purchased for injection in the field decreased with time for the particular well design.

The total annual operating cost was given as:

$$C_{OPEX} = \text{O\&M}^t_{annual} = \text{O\&M}^t_{daily} + \text{O\&M}^t_{cons} + \text{O\&M}^t_{sur} + \text{O\&M}^t_{subsur} + \text{C}^t_{rec} + \text{C}^t_{CO_2} + \text{C}^t_{Water} \quad (13)$$

A summary of the important CAPEX and OPEX components, and any assumed reference value is shown in Tables 5 and 6, respectively.

Table 5. Components of Operating Expenditure

Variable	Value	Comments/ References
Fixed OPEX (%)	5	Fixed OPEX is 5% of CAPEX (Lawal, 2011; Wei et al., 2015)
	Variable OPEX	
Gas Injection ($/ MMscf)	580	(Gaspar Ravagnani, Ligero, & Suslick, 2009; Neal, Hou, Allinson, & Cinar, 2010)
CO_2 Capture, ($/ MMscf)	1600	(Gaspar Ravagnani et al., 2009; Nogueira & Mamora, 2005).
CO_2 Compression Cost, ($/ t CO_2)	The mean cost of 13USD/t for 1Bar of CO_2 and 1USD/t for high pressured gas from a pipeline terminal were applied.	Wei et al., (2015)
CH_4 Treatment, ($/ MMscf)	400	A value of 20% of sale gas price was assumed Wei et al., (2015).
Fluid Handling/ Treatment, ($ /stb)	1 for oil and water pumping, and 12 for oil treatment.	(National Energy Board of Canada (NEB), 2006)
Water Compression and Injection, ($ /m^3)	1.2 for a WAG process regardless of pressure difference	Anthony and Mohan, (2010); Wei et al., (2015)
CO_2 recycling cost, ($/ t CO_2)	$C_{rec} = 23.66 \cdot Q$	Wei et al., (2015); Tayari et al., (2015)
Daily and Consumables O & M Costs, $/annum	Daily O&M = N_{well} x 7596. Cons. O&M = N_{well} x 20,295	Wei et al., (2015)
O & M cost for well facilities, $/annum	$O\&M_{sur} = N_{well}$ x 15420 x $[(d/(280 \times N_{well}))^{0.5} + 5000]$; $O\&M_{subsur} = N_{well} \cdot [5669 \cdot (d/1219)]$	Wei et al., (2015)

Table 6. CAPEX Components

Variable	Value	Comments/ References
Drilling and Completions		
Number of new injection wells	1	-
Number of new production wells	2	-
Cost (10^6 USD/well)	1.5	Tayari et al., (2015)
Surface Pipelines/Flowlines		
Number of injection lines	1	One flowline per injector
Number of new production lines	2	One flowline per producer
Length per line (km)	1	
Cost (10^6 USD/well)	0.5	Tayari et al., (2015); Cremon et al., (2020)
Processing Facilities		
Peak water rate (10^3 stb/d)	3	Based on the secondary waterflood (Ogbeiwi et al., 2020b)
Peak liquid rate (10^3 stb/d)	5	Based on the secondary waterflood (Ogbeiwi et al., 2020)
Cost of liquid facilities (10^6 \$ / 10^3stb liquid)	1.9	Wang et al., (2018)
CO_2 Capture and Compression Facilities		
Peak gas rate (10^6 scf/d)	1	This rate will decrease across the project's lifecycle since produced CO_2 will be recycled.
Peak CO_2 injection rate (10^6 scf/d)	1	This rate is dependent on the gas cycle time of CO_2 injection.
Unit cost of capture (10^6 \$ / 10^6scf)	13	The CAPEX of a post-combustion capture process is approx. 10x that of compression (Hill, Hovorka, & Melzer, 2013; Kazeem Akintayo Lawal, 2011).
Unit compression cost 10^6 USD / MMscf)	1.3	Gaspar Ravagnani et al., (2009)
Other Components		
CAPEX contingency (%)	10	Assumption (Shell, 2001)
Decommissioning cost (% of CAPEX)	25	(Kemp & Stephen, 2015; Welkenhuysen, Meyvis, & Piessens, 2017)
CAPEX phasing (% / year)	100	CAPEX spending calculated for the first year.

4.2. Revenues and Penalties. Two sources of revenue were explored in this study:

a. The principal revenue source was earnings from the sale of recovered hydrocarbons (oil and gas).
b. Revenues could be made as a result of the safe storage of CO_2 that would otherwise have been released into the atmosphere. This was referred to as a carbon credit.

The economic model also predicted that any fugitive carbon emissions would result in penalties. This means that any stranded CO_2 was subject to a carbon tax. Table 7 shows the revenue and rates of carbon penalties as a reference.

Table 7: Components of Revenue and Penalty

Item	Rate	Comments/ References
Oil Price, USD/stb	70	Bloomberg, (2022)
Gas price, USD /MMscf	2000	Mokhtari et al., (2016); Hill et al., (2013)
Carbon Credit, USD /ton CO_2	16	Mokhtari et al., (2016)
Carbon Penalty, USD /ton CO_2	60	IHS MARKIT, (2016)

Yearly revenues were calculated by estimating the annual hydrocarbon output and gas storage. Because the produced gas was more than 80% CO_2 at the time, the earnings from the sale of produced gas decreased dramatically after three years of CO_2 injection. As a result, the two principal sources of revenue were oil sales and carbon credits. The price of West Texas Intermediate (WTI) oil rose from $60 per barrel (in 2019 USD) to $100 in 2022, according to the Annual Energy Outlook (AEO), 2021 reference case. However, because crude oil prices are affected by a variety of factors, a low price of $50 was used as the minimum price, and a high price of $80 was utilised as the maximum price. In the deterministic analysis, an average price of $70 per barrel, which was the average between 2019 and 2022, was used for economic assessment. Sensitivity analysis was performed using 50-80 USD/bbl, which simulates changes in crude oil prices.

4.3. Fiscal Policy. The Nigerian government operates three additive tax regimes in its upstream petroleum sector: the corporation tax, the Petroleum Technology Development Fund (PTDF) tax, and the Tertiary Education Trust Fund (TETFund) tax (Kazeem Akintayo Lawal, 2011). Table 8 shows the reference values for these fiscal terms.

Table 8. Components of Fiscal Terms

Term	Value	Comments/ References
Corporate tax, %	30	CITA, (2004); PPT, (1990)
PTDF Tax, %	3	PTDF, (1990)
TETFund Tax, %	2	ETF, (1993)
Depreciation, %	20	NIPC, (2010)

Royalty, %	8	PPT, (1990)
Discount Rate, %	10	Yang et al., (2007)

The royalty rate in the Niger Delta varies by reservoir location, and it is also affected by the type and amount of hydrocarbons produced, as well as the price of oil (Echendu & Iledare, 2016; PIB, 2009). The royalty for offshore basins, to which the case study reservoir belongs, is 8.0%. As a result, we applied this value to hydrocarbon royalties as well as any oil and gas price. Table 11 shows the royalties for the various Niger Delta basins. The differential in fiscal rates between these sites is one of the Nigerian government's measures to entice investors to explore its offshore assets (Onwuka et al., 2012; Echendu and Iledare, 2016). Table 9 shows the royalty conditions of Production Sharing Contracts (PSCs) by location.

Table 9. Production Sharing Contracts (PSCs) royalty provisions by location

Royalties (%)						
Max. Water Depth (m)	100	200	500	800	1000	> 1000
Swamp/Shallow	18.5					
Shelf		16.5				
Deep			12.0	8.0	8.0	8.0

In this study, we followed the Nigerian government's specification (NIPC, 2010), which calls for a straight-line depreciation technique to account for asset depreciation. Specifically, the capital expenditure items were depreciated equally throughout the first three years after incurring the expenditure (Kazeem A Lawal, 2011; Onwuka et al., 2012).

4.3. Parametric Studies, Sensitivity and Uncertainty Analysis. We assessed the influence of the project's uncertain economic factors on its net present value (NPV). Table 10 illustrates the design parameters used in this study as well as the range of uncertainty for each parameter. The uncertainties in the offshore Niger Delta hydrocarbon province's tax regimes and fiscal policy were neglected because these are government policies and are not subject to change like the CAPEX and OPEX variables,

The uncertainty range for each parameer was established using the existing economics of Nigeria's hydrocarbon industry and other previously stated assumptions. Because there are no

CO_2 EOR projects in the Niger Delta, the absence of carbon credits was believed to be the worst-case situation, while revenue of 20 USD per tonne of CO_2 stored was supposed to be the best-case scenario. Furthermore, given the lack of a ready market for the purchase of produced CH_4 and lighter hydrocarbons, we projected that in the worst-case scenario, no revenue would be generated from the sales of the produced gas, and that all of it would be converted to CO_2 for injection or flared as undesired gas. Finally, to account for inflation, we assumed a maximum change of 30% in the cost of CO_2 recycling and other unit operations and capital expenditure (CAPEX).

Table 10. Economic Uncertainties and their ranges.

Economic Variable	Low	Median	High
Oil Price, $/stb	50	70	80
Discount Rate, %	5	10	15
Carbon Credit, $/ton CO_2	0	10	20
Gas (CH_4) price, $/MMscf	0	2000	2500
Change in CO_2 recycling cost	0	10	30
CO_2 injection cost, $/MMScf	580	1000	2000
% Change in unit OPEX cost	0	10	30
Increase in CAPEX, %	0	10	30

The percentage contribution of each variable to changes in the values of the objective function was used to illustrate the variables' influence on the objective function. The impacts of the various factors on the objective function were calculated as the percentage contribution of each variable, which is provided as:

$$\%\ contribution = \frac{|Y_{i,max} - Y_{i,min}|}{\Sigma|Y_{i,max} - Y_{i,min}|} \times 100\% \qquad (15)$$

Where $Y_{i,max}$ and $Y_{i,min}$ are the maximum and minimum values of the objective function(s) evaluated for the minimum and maximum values of each economic variable *i*, respectively. The denominator represents the sum of the numerator for all the variables.

The sensitivity analysis does not adequately follow and depict the behaviour of the project's value, especially when numerous input parameters are changed at the same time. Furthermore, more than conventional sensitivity analysis is required to effectively address and quantify the effect of uncertainty resulting from the complexities of investment decisions (Welkenhuysen, Rupert, et al., 2017). This is especially important when the input parameters

follow a specific trend, such as a probability distribution function (Ghaderi, Clarkson, Taheri, & Chen, 2013). In this instance, the value of the desired objective function (the NPV in this case) would most likely be biased towards undesirable, risky values across diverse combinations of the input variables. The uncertain attributes of the NPV objective function can be generated using Monte Carlo simulations (MCS), which can then be merged by assigning an appropriate probability distribution function to each uncertain variable (Cremon, Christie, & Gerritsen, 2020b; Jia, McPherson, Pan, Dai, & Xiao, 2018).

In this study, Monte Carlo simulations on the NPV objective function were done to analyse the related risk of failure or success of the flooding project under economic uncertainty and to provide a basis for the CO_2 flooding project. The Monte Carlo simulation (MCS) is a simple yet effective method for dealing with stochastic uncertainty (Cunha, 2007). It uses a random sampling of the uncertainty or uncertainties within its or their set ranges to provide the user or engineer with multiple outcomes. To represent the uncertainty in the input data, a uniform probability distribution function was assigned to each economic variable using the low, median, and high values as described by Ghaderi et al., (2013). Table 6.9 shows the range of uncertainties for the economic metrics. Ten thousand Monte Carlo simulations were used to create a cumulative distribution function of the NPV response.

To create samples of economic uncertainties for the uncertainty analysis, we used the Latin-Hypercube experimental designs. The Latin-Hypercube design is a pseudo-Monte Carlo sampling design that uses stratified sampling in its construction, requiring the search algorithm to be optimal (Helton & Davis, 2003). Because the values of each parameter sample are consistently created from a multidimensional distribution, every part of the range of the unknown variable is well represented in the sample generated by design in this design. As a result, for sampling during uncertainty analysis, the Latin-Hypercube design is superior to standard experimental design strategies such as the Box-Behnken design, central composite design, and so on (Helton & Davis, 2003; Montgomery, 2008).

Figure 7 summarises the technique used in this work to assess the possibility of CO_2 EOR and storage in the Niger Delta.

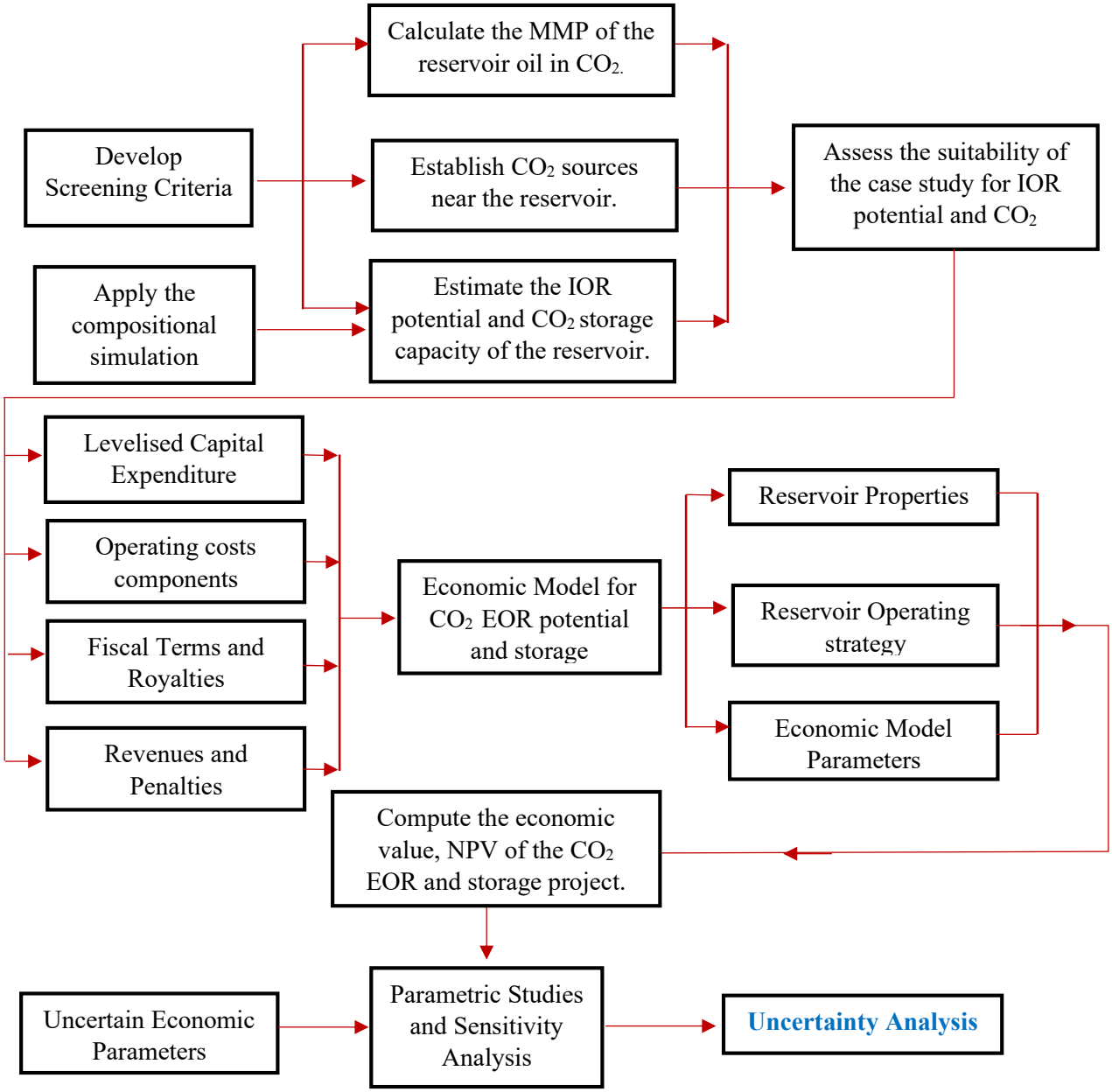

Figure 7. Methodology for assessing the potential of CO_2 EOR and storage in the Niger-Delta.

5 RESULTS AND DISCUSSION

5.1. Screening Criteria for CO_2 EOR and storage. Different studies have proposed different criteria for screening reservoirs for CO_2 EOR and storage, as indicated in Table 11. The proposed criteria for this study were established by considering screening criteria from expert studies on miscible CO_2 floods. Table 11 shows these criteria, which were trimmed from Table 1 and the reservoir case study features. Based on the first screening results, the reservoir offers a high potential for CO_2 EOR and storage. We then used material balance volumetric calculations and numerical simulations to estimate these potentials.

Table 11. The Screening Criteria for CO_2 miscible flooding and the criteria used in this study.

Parameter	Oil density (g/cm^3)	Oil gravity (^{o} API)	*Pi* (MPa)	T (^{o}C)	μ (mPa.s)	*K* (mD)	S_o	Depth (m)
Carcoana (1982)	< 0.8227	> 40	> 8.3	< 90	<2	> 1	>0.30	< 3000
Taber, (1983)	< 0.8948	>26			<15		>0.30	>700
Klins, (1984)	< 0.8762	>30	>10.3		<12		>0.25	>914
Ren, (2008)	0.9218 – 0.7587	22 – 55		<120	<188	>5	0.28 – 0.64	600 – 3500
Zhao, (2001)	< 0.9218	> 22			<10		>0.20	
Bachu, (2004)	0.8924 – 0.7883	27 - 48	>7.5	32 – 120			>0.25	
This Study	< 0.93	>22	>7.5	32 – 120	<188	>1	>0.20	600 – 3500

Table 12 presents some specific properties of the reservoir. A comparison of Tables 11 and 12 shows that the properties of the reservoir are within the range required for a reservoir to be considered for CO_2 miscible flooding for EOR and carbon storage.

Table 12. The properties of this reservoir showing its suitability for CO_2 miscible flooding.

Reservoir Property	*This Study*
Permeability, *K* (mD)	700
Initial reservoir pressure, P_R (psia)	1950 (13.45 MPa)
Initial reservoir temperature, ^{0}F	165 (73.9 ^{o}C)
Oil Viscosity, μ_o (cP)	0.31
Oil Density, ρ_o (lb/ft^3)	57.98 (0.924 g/cm^3)
Reservoir Depth (ft)	4450 (1356.4 m)

5.2. Estimates of the Potential for Enhanced Oil Recovery and CO_2 Storage. The pore volumes, incremental oil recovery, and CO_2 storage capacity of the case study reservoir were evaluated using reservoir fluid volumes-in-place before and after the waterflood, as well as fluid volumes produced. Following the secondary production stage, these volumes were generated from the reservoir simulation model, and the gas total volume estimates included

both free and dissolved gas volumes. At the end of the secondary flooding, approximately 47.839 MMSTB of oil had been produced, representing approximately 58% of the original oil reserves. Table 13 summarises the reserve estimations following flooding.

Table 13. Summary of the reserve estimates at the end of the waterflooding at surface conditions.

Volumes	Oil (x 10^6 stb)	Water (x 10^6 stb)	Gas (x 10^6 Mscf)
Currently in Place	34.567	38614.504	13.126
Produced	47.839	85.496	19.157
Originally In Place	82.406	38700	32.283

The total volume of oil in the reservoir was approximately 82.406 MMSTB, with 47.839 MMSTB produced after primary production and the flood. At the end of secondary production, the total gas volume was 32.283 x 10^6 Mscf, with 19.157 x 10^6 Mscf recovered. The reservoir's theoretical and effective storage capacity were then calculated based on current hydrocarbon (gas and oil) and water production data at the end of the waterflood (converted to metric units at the surface conditions for conformity). Table 14 shows the reservoir reserve estimates at the end of the waterflooding in m^3.

The reservoir's technical and effective storage potentials, as well as its incremental oil recovery potential, were then calculated using Equations 5 - 8. The CO_2 storage capabilities were calculated at subsurface circumstances, but the additional oil recovery was calculated at surface conditions.

Table 14. Summary of the reserve estimates at the end of the waterflooding in m^3 at reservoir conditions.

Volumes	Oil	Water	Gas
Currently in Place	6.24	6206.35	475.15
Produced	8.64	13.74	693.43
Originally In Place	14.88	6220.09	1168.58

Table 15 highlights the estimations of technical and effective storage capacity, as well as incremental oil recovery following CO_2 flooding. In summary, the theoretical and effective storage capacities at reservoir conditions were 514.57 x 10^6 t of CO_2 and 192.96 x 10^6 t of CO_2, respectively, or 404.64 x 10^6 t of CO_2 and 151.74 x 10^6 t of CO_2, respectively. The incremental oil recovery potentials for the effective and theoretical estimates were 14.91 x 10^6 and 11.18 x 106 sm_3 of oil, respectively.

Table 15. Summary of technical and effective estimations of storage capacity and incremental oil recovery following CO_2 flooding.

Quantity	Technical Estimate	Effective Estimate
Storage capacity (x10^6 t)	514.57	192.96
Incremental Oil Recovery (x 10^6 sm^3)	14.91	11.18

We applied the numerical simulation of miscible CO_2 flooding to the case study reservoir to present more realistic and accurate assessments of the reservoir's potentials. The CO_2 gas was continuously injected for 24 years before the wells were shut down and production and injection ceased. The total amount of gas and oil recovered was then used to calculate the effective carbon storage and increased oil recovery potentials. After 24 years of continuous CO_2 injection, the volume of CO_2 stored, and incremental oil recovered are depicted in Figure 8. Because the injected gas began to undergo considerable breakthroughs at the production wells, the amount of CO_2 stored in the subsurface increased steadily from the start of injection until after 0.6 HCPV of gas had been injected. At this point, the efficient sweep of the reservoir oil by the pre-breakthrough injected CO_2 had provided more than half of the cumulative oil recovery experienced during the CO_2 flooding experiment. At the end of the injection period, about 1.72 HCPV of CO_2 gas was injected, approximately 1.23 x 10^9 Mscf of CO_2 (or 34.82 x 10^9 sm^3) was stored, and approximately 18.23 MM STB (or 2.898 x 10^6 sm^3) of oil was produced.

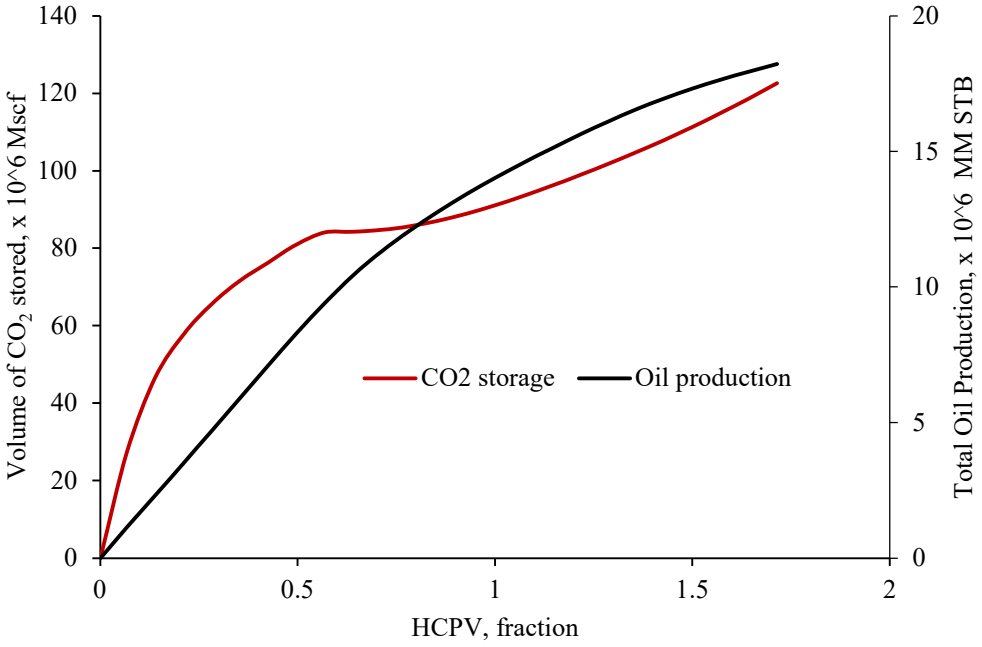

Figure 8. Cumulative volume of Gas stored, and oil produced after 24 years of continuous CO_2 injection.

5.3. Sensitivity Analysis. Figure 9a depicts the findings of the preliminary screening analysis. The most significant economic uncertainty was the price of the produced oil, with its volatility accounting for more than 60% of variations in the project's value. The cost of CO_2 injection and the discount rate are two other major economic uncertainties. The fluctuation in the NPV was primarily due to changes in capital costs.

By adjusting one parameter at a time, the sensitivity of the economic uncertainty to the NPV response shown in Figure 8b was determined. The NPV increased from 382.83 to 445.64 million USD when the oil price rose from 50 to 80 USD/stb. Furthermore, a change in the operating cost of CO_2 injection reduced the project's value by 5.35%, from 425.63 million USD to 402.84 million USD. The changes in CAPEX and CO_2 recycling costs had the least impact on the NPV, with each variable resulting in a 0.15% decline in the project's value. Other revenue streams, such as carbon credits and gas sales, had extremely tiny effects when compared to the influence of oil prices. As a result, even without these earnings, the project was still profitable at an oil price of 50 USD/stb. Figure 9 depicts the influence of the other variables.

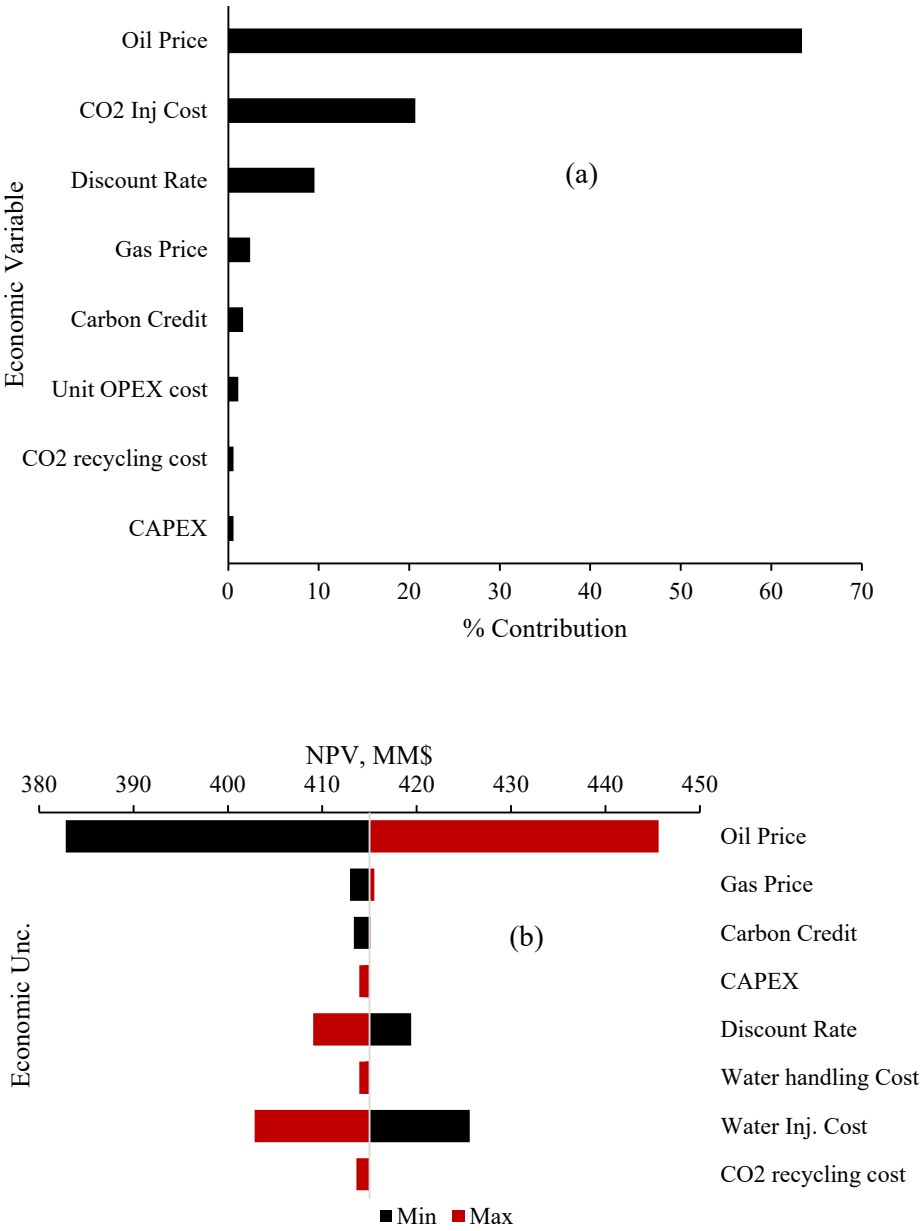

Figure 9. (a) Pareto charts and (b) results of the sensitivity studies showing the key economic uncertainties impacting NPV.

5.4. Uncertainty Analysis. The probability and cumulative distribution functions of the NPV of the CO_2 flooding project over the range of uncertainty of the economic variables were then generated by applying 10,000 combinations of Monte Carlo samples of the economic parameters to the NPV of the flooding project. Figure 10(a) depicts the probability distribution function of the NPV of the CO_2 storage project in the reservoir when the economic parameters' values were uncertain. Under uncertainty, the average cost of the CO_2 EOR and sequestration project was 414.24 million USD, with a standard deviation of 19.652

million USD, a minimum cost of 366.69 million USD, and a maximum cost of 461.58 million USD.

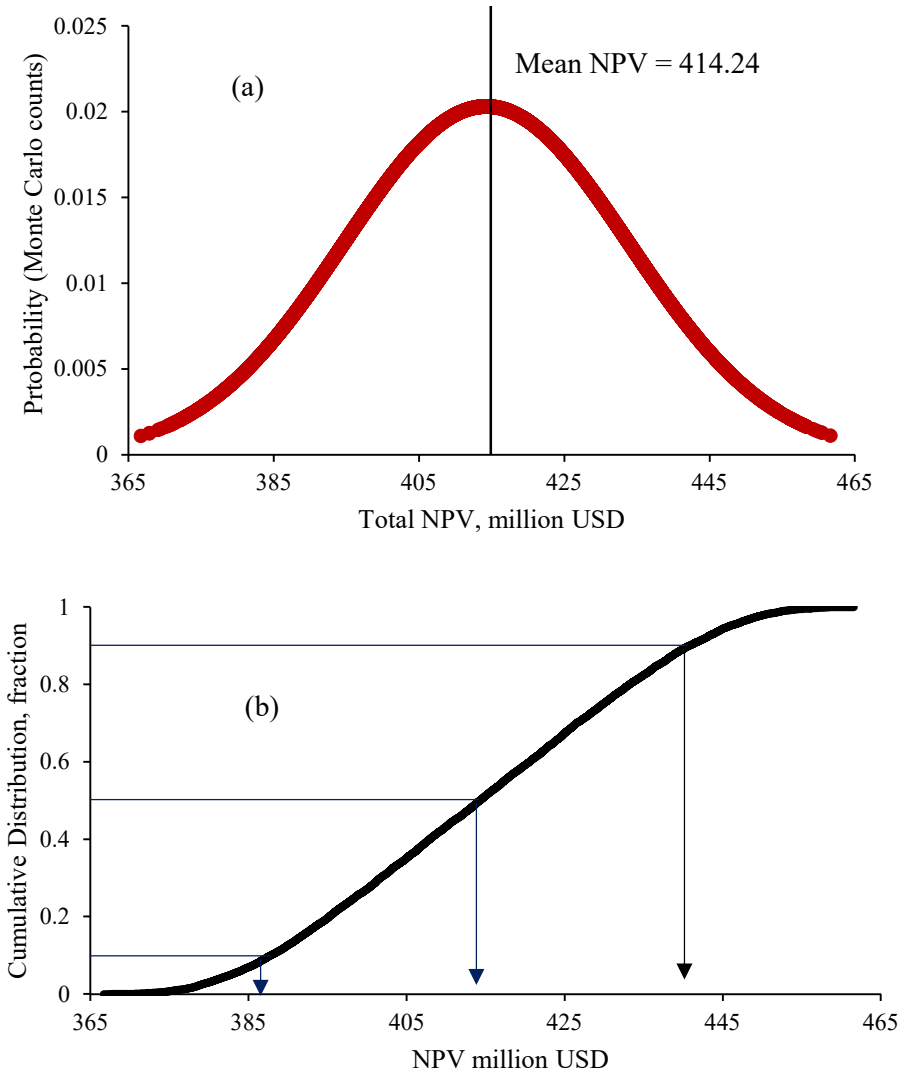

Figure 10. The (a) probability distribution function (PDF), and (b) cumulative distribution function (CDF) of NPV after the CO_2 flood, showing the P10, P50, and P90 NPV values.

Figure 10(b) depicts the Gaussian-like behaviour of the CDF of NPV following the CO2 flood. The 10th, 50th, and 90th percentiles of the NPV were 387.79, 414.24, and 440.74 million USD, respectively. According to Welkenhuysen et al., (2017b), the spread in the NPV from the P10 to the P90 from the deterministic value, i.e., the mean or P50, was detected from the CDF plot, suggesting the presence of uncertainty in the forecast of the economic value of the CO_2 flooding project.

Figure 11 depicts the variations in the project's net cash flow (NCF) with time for different price scenarios. For example, at the lowest price of 50 USD/stb, the net income ranges from

approximately -39 million USD in the first year to approximately 117 million USD in the sixth year. In the case study, the project reaches break-even and becomes cost-effective (with NCF > 0) after the first year (particularly, 0.5 years) of CO_2 flooding and injection of 0.03 HCPV of CO_2. This was due in part to relatively modest initial capital expenditures (CAPEX) due to existing infrastructure such as wells, pipelines, separators, and so on, as well as large revenue from the sale of incremental oil recovery. The annual cash flow from the project increased steadily until the end of the seventh year, during which time approximately 0.6 HCPV of gas was injected, 9.41 MMSTB of additional oil produced, and 8.41 x 10^9 ft^3 of carbon was stored.

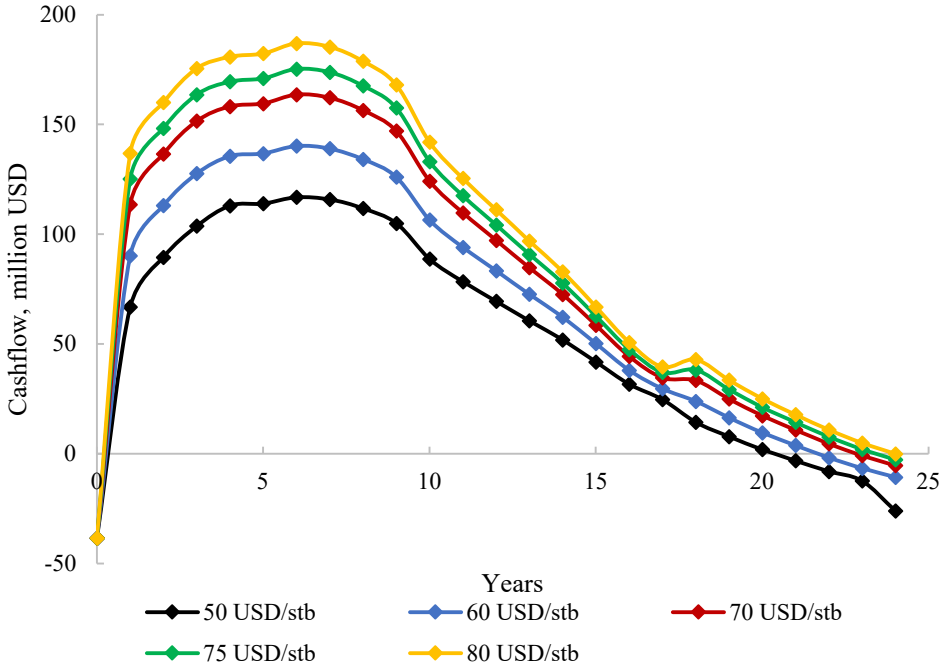

Figure 11. Changes in the net cash flow (NCF) of the project with time at different price scenarios.

Following this period, a gradual fall in project income was observed due to a breakthrough of the injected gas at the producers, resulting in increased gas production and decreased oil production. As a result, revenue from oil recovery decreased while expenditures related with CO_2 treatment and recycling increasing. The project became unprofitable after 20 years of CO_2 injection as the NCF < 0, and the costs expended in years 23 and 24 were decommissioning and other associated costs. In conclusion, regardless of oil price, CO_2 EOR and storage in the Niger-Delta reservoir are economical and have a positive cash flow between Years 1 and 20 as long as oil prices remain over 50 USD/barrel. Trends similar to this are observed at other oil prices.

6. CONCLUSIONS

Using the properties of a turbidite case study reservoir, we investigated the feasibility for CO_2-enhanced oil recovery and storage in the Niger Delta. To analyse the potential of the case study reservoir for CO_2 EOR and storage, we first established and implemented screening criteria. The preliminary screening studies reveal that the reservoir's properties make it appropriate for miscible CO_2 injection. The storage and additional oil recovery potentials of the site were then assessed using analytical and numerical simulation methods. The volumetrics of the case study reservoir simulation model were used to calculate the analytical technical and effective potentials for miscible CO_2 flooding for CO_2 storage and EOR. The reservoir possesses technical and effective CO_2 storage potentials of 514.57 and 192.96 metric tonnes of CO_2, as well as technical and effective incremental oil recovery potentials of 14.91 and 11.18 x 10^6 sm^3 of oil, according to the results obtained.

We used numerical simulations to calculate the site's CO_2 storage and incremental oil recovery potentials after 24 years of continuous CO_2 injection to account for the factors that influence the dynamics of the CO_2 flooding process and for more realistic capacity estimates. According to the results of this evaluation, approximately 6.7 HCPV of gas had been injected at the end of this period, storing approximately 45 x 10^6 Mscf of CO_2 (or 1.274 x 10^9 sm^3) in the subsurface and producing 7.85 MM STB (or 1.248 x 10^6 sm^3) of oil.

We created and utilised a novel economic model for the CO_2 EOR process in the Niger-Delta case study to evaluate the project's net present value (NPV) to determine the commercial viability of the CO_2 flooding project. The developed cost-economic model incorporated expenses, revenue factors, and fiscal terms available in the Niger-Delta hydrocarbon province. The economics and commercial risk of the CO_2 flooding project were also evaluated using an approach that combined sensitivity analysis, experimental design, and used Monte-Carlo-simulation-based uncertainty analysis. According to the evaluation results, the oil price is the most important determinant of the project's economic performance and profitability.

In conclusion, the evaluation results demonstrated that the case study reservoir in the Niger Delta Basin is a suitable location with enormous potential for CO_2 EOR and storage. The technique used and the results obtained could be utilised in decision-making for future carbon emission reduction programmes in the Niger Delta oil region. Furthermore, the method

utilised in the study can be used to assess the potential for CO_2 EOR and storage in other petroleum basins.

7. ACKNOWLEDGEMENTS

The authors would like to express their gratitude to the Petroleum Technology Development Fund (PTDF) for supporting this research. Schlumberger is also credited for providing the ECLIPSE 300 simulator, which was employed in this investigation.

8. AUTHOR INFORMATION

The work was funded by the Petroleum Technology Development Fund (PTDF), Grant No.: PTDF/ED/PHD /OP/1348/18.

The authors declare no competing financial interest

9. DATA AVAILABILITY

The datasets generated during and/or analysed during the current study are available from the corresponding author on reasonable request.

10. APPENDIX

Analysis of the volumes of gas recovered and gas flared in reservoirs of the Niger-Delta petroleum basin (after Umar et al., 2020)

S/N	Oil Field	Gas Production (x 10^6 Mscf)	Flaring (x 10^6 Mscf)	% of produced gas that is flared
1	Adibawa	2.23	2.1	94.54
2	Afam	19.47	0.28	1.43
3	Afremo	3.22	3.21	99.72
4	Agbaya	3.16	3.11	98.49
5	Ajitaton	0.54	0.53	98.05
6	Akaso	11.61	8.73	75.18
7	Alakiri	6.12	3.66	59.77
8	Amukpe	0.08	0.07	92.1
9	Awoba	13.36	6.6	49.37
10	Belema	11.94	11.83	99.08
11	Benisede	4.47	4.35	97.45
12	Bonny	92.94	0.74	0.79

13	Diebu Creek	15.79	15.68	99.3
14	Ekulama	12.25	12.13	99.06
15	Elelenwa	6.05	1.66	27.51
16	Eriemu	5.11	5.07	99.15
ss17	Escravos Beach	4.3	2.87	66.69
18	Etelebou	4.49	4.28	95.41
19	Kanbo	5.3	5.16	97.4
20	Kolo Creek	43.14	0.99	2.29
21	Krakama	9.66	9.34	96.68
22	Nembe Creek	14.65	0.93	6.35
23	Nun River	3.6	3.53	98.23
24	Obigbo North	24.01	7.01	29.18
25	Opukushi	8.29	8.1	97.69
26	Oroni	0.61	0.59	95.36
27	Otumara	8.07	8	99.16
28	Saghara	0.81	0.81	100
29	Soku	189	3.64	1.93
30	Tunu	12.44	12.28	98.76
31	Adua	11.32	9.49	83.81
32	Asabo	24.15	15.88	65.75
33	Ekpe	4.89	0.55	11.23
34	Eku	3.53	2.56	72.54
35	Enang	10.35	2.8	27.05
36	Etim	21.45	14.22	66.3
37	Inim	80.03	1.5	1.88
38	Usari	65.41	3.31	5.06
39	Okan	78.3	11.97	15.28
40	Mefa	51.81	2.56	4.94
41	Robertkiri	14.11	14.05	99.58
42	Yorla South	0.77	0.75	97.4
43	Belema Unit	0.01	0.01	100
44	Obagi	27.1	13.87	51.18
45	Odudu	8.7	7.33	84.2

46	Ebocha	54.46	47.07	86.43
47	Oshi	40.72	33.8	83
48	Tebidaba	10.74	10.66	99.31
49	North Apoi	6.31	6.27	99.29
50	Ologbo	18.03	16.87	93.57
51	Ossiomo	8.89	8.89	100
52	Agbara	9.66	9.36	96.83
53	Jones Creek	7.86	7.71	98.07
54	Odidi	18.63	12.22	65.6
55	Opuama	0.73	0.01	0.72
56	Oben	36.67	12.45	33.95
57	Odeama Creek	12.84	2.92	22.75
58	Orubiri	5.13	5.13	100
59	Ovhor	1.35	1.25	92.73
60	Sapele	25.25	10.51	41.61
61	Ubefan	0.12	0.12	99.44
62	Middleton	1.89	1.89	100
63	Pennington	2.07	2.05	98.76
64	Oso	182	22.22	12.19
65	Forcado Yokri	12.85	12.31	95.8
66	Akono	0.43	0.42	97.51
67	Egbema	5.14	5.11	99.49
68	Batan	3.01	2.92	96.83
69	Egwa	11.57	10.21	88.26
70	Oguta	14.75	14.72	99.74
71	Olomoro	5.02	3.81	76.03
72	Ubie	87.56	2.28	2.6
73	Uzere West	2.1	2.05	97.42
74	Oweh	2.82	1.08	38.2
75	Clough Creek	0.95	0.89	93.47
76	Biseni	2.28	2.11	92.49
77	Obodo	0.69	0.4	58.97
78	Aghigho Creek	0.44	0.34	75.57

79	Ibewa	61.41	0	0
80	Ajuju	0.4	0.28	71.49
81	Afiesere	9.42	9.07	96.26
82	Ahia	4.88	4.85	99.25
83	Evwreni	1.05	0.96	90.85
84	Imo River	7.95	7.05	88.76
85	Isoko	1.1	0.93	84.45
86	Rumuekpe	0.39	0.37	94.97
87	Kokori	3.36	3.1	92.27
88	Utorogu	89.26	1.65	1.84
89	Eriemu	5.11	5.07	99.15
90	Ughelli East	17.77	0.71	4
91	Ughelli West	1.26	1.22	96.79
92	Osiaka	0.07	0.01	8.38
93	Warri river	0.02	0.02	97.13
94	Ogini	1.47	0.91	62.09
95	Beniboye	7.22	7.16	99.13
96	Malu	8.76	8.72	99.52
97	Edican	5.25	5.25	100
98	Abiteye	4.49	0.32	7.02
99	Oredo	5.9	5.45	92.42
100	Meji	27.06	7.83	28.95
101	Abo	0.84	0.78	92.75
102	Oyo	0	0	75.34
103	Gili-Gili	0.82	0.81	99.34
104	Funiwa	11.11	11.06	99.51
105	Okubie	2.33	2.33	100
106	Obama	18.01	17.57	97.55
107	Afia	1.73	1.73	100
108	Odudu	8.7	7.33	84.2
109	Ofon	19.41	18.91	97.37
110	Erha	59.29	2.62	4.41
111	Omuro	0.6	0.59	97.29

112	Jisike	2.29	2.28	99.53
113	Okono	15.22	14.66	96.33
114	Asaboro South	1.45	1.45	100
115	Ogharefe	3.67	3.67	100
116	Ologbo	18.03	16.87	93.57
117	Ossu	6.05	5.97	98.7
118	Bonga	36.5	4.23	11.58
119	Awawa	5.25	0.76	14.39
120	Yoho	32.94	10.1	30.66
121	EA	18.71	10.29	55
122	Parabe	12.94	12.78	98.71
123	Mina	1.38	1.38	99.97
124	Tapa	3.67	3.62	98.4
125	Delta	23.55	23.47	99.66
126	Eja	1.55	0.76	48.84
127	Asabo	24.15	15.88	65.75
128	Akri	27.58	19.54	70.82
129	Edop	51.51	20.24	39.29
130	Asasa	26.2	20.42	77.95
131	Idu	18.08	17.9	99.01
132	Olo	4.81	0	0.07
133	Otamini	1.99	1.9	95.56
134	Graban	75.56	1.57	2.08
135	Isan	2.14	2.1	97.9
136	Jokka	0.72	0.72	100
137	Ogbotobo	4.78	4.71	98.45
138	Benin River	0.72	0.72	100
139	Gbokoda	4.78	4.71	98.45
140	Makaraba	12.81	1.19	9.29
141	Kito	0.45	0.43	95.61
142	Dibi	13.07	6.29	48.13
143	Delta South	17.1	10.03	58.65
144	Mini NTA	7.33	7.29	99.39

145	Umuechem	1.92	1.91	99.06
146	Santa Barbara	3.79	0.77	20.44
147	Cawthorne Channel	32.19	24.43	75.91
148	NDA	3.57	2.21	62.04
149	Okwori	10.4	7.14	68.69
150	Abura	1.98	1.27	64.06
151	Isimiri	3.15	2.7	85.56
152	Nkali	7.41	2.88	38.88
153	Ubit	54.38	5.43	9.98
154	Mimbo	3.26	2.55	78.22
155	Ebughu	9.11	8.34	91.61
156	Akam	4.6	3.92	85.24
157	Ukpam	0.45	0.39	87.83
158	Iyak SE	1.44	0.94	65.16
159	Inanga	3.05	2.32	76.1
160	Mfem	1.38	1	72.42
161	Isobo	3.03	3.03	100
162	Unam	7.33	6.2	84.53
163	Idoho	11.15	11.11	99.67
164	Utue	3.09	2.66	86.14
165	Iyak	9.24	4.52	48.9
166	Ime	3.15	2.84	90

11. REFERENCES

Adegoke, O. ., Petters, S. ., Fayose, E. A., Oyebamiji, A. S., Ajisafe, I. K., Tiamiyu, A. I., … O. Ogunjobi. (2017). *Cenozoic Foraminifera and Calcareous Nannofossil Biostratigraphy of the Niger Delta, chapter 2 Geology of the Niger Delta Basin*. https://doi.org/10.1016/B978-0-12-812161-0/00002-8

Aghdam, K. A., Moghaddas, J. S., Moradi, B., Dabiri, M., & Hassanzadeh, M. (2013). Maximizing the oil recovery through miscible Water Alternating Gas (WAG) injection in an Iranian oil reservoir. *Petroleum Science and Technology*, *31*(22), 2431–2440. https://doi.org/10.1080/10916466.2011.569822

Ahmadi, M. A., Zendehboudi, S., & James, L. A. (2017). A reliable strategy to calculate minimum miscibility pressure of CO2-oil system in miscible gas flooding processes. *Fuel*, *208*, 117–126. https://doi.org/10.1016/j.fuel.2017.06.135

Al-Mudhafar, W. J., Rao, D. N., & Srinivasan, S. (2018). Robust Optimization of Cyclic CO2 flooding through the Gas-Assisted Gravity Drainage process under geological uncertainties. *Journal of Petroleum Science and Engineering*, *166*(March), 490–509. https://doi.org/10.1016/j.petrol.2018.03.044

AL-Muftah, A., BuAli, Y., Mahmoud, A., & AlGhadhban, H. (2019). *Simulation and Performance of Immiscible WAG Pilots in Mauddud Reservoir Using Three Phase Relative Permeability with Hysteresis*. https://doi.org/10.2118/195103-ms

Aminu, M. D., Nabavi, S. A., Rochelle, C. A., & Manovic, V. (2017). A review of developments in carbon dioxide storage. *Applied Energy*, *208*(August), 1389–1419. https://doi.org/10.1016/j.apenergy.2017.09.015

Anthony, E. P., & Mohan, A. (2010, June 27). Water Management vs. Water Control: Profitability, Not Cost, Driving the Paradigm Change. *Trinidad and Tobago Energy Resources Conference*, p. SPE-132253-MS. https://doi.org/10.2118/132253-MS

Arinkoola, A. O., & Ogbe, D. O. (2015). Examination of Experimental Designs and Response Surface Methods for Uncertainty Analysis of Production Forecast: A Niger Delta Case Study. *Journal of Petroleum Engineering*, *2015*, 1–16. https://doi.org/10.1155/2015/714541

Arinkoola, A. O., Onuh, H. M., & Ogbe, D. O. (2016). Quantifying uncertainty in infill well placement using numerical simulation and experimental design: case study. *Journal of Petroleum Exploration and Production Technology*, *6*(2), 201–215. https://doi.org/10.1007/s13202-015-0180-z

Arogundade, O. A., Shahverdi, H.-R., & Sohrabi, M. (2013). *A Study of Three Phase Relative Permeability and Hysteresis in Water Alternating Gas (WAG) Injection*. 1–16. https://doi.org/10.2118/165218-ms

Assef, Y., Kantzas, A., & Pereira Almao, P. (2019). Numerical modelling of cyclic CO2injection in unconventional tight oil resources; trivial effects of heterogeneity and hysteresis in Bakken formation. *Fuel*, *236*(August 2018), 1512–1528. https://doi.org/10.1016/j.fuel.2018.09.046

Bachu, S. (2003). Screening and ranking of sedimentary basins for sequestration of CO2 in geological media in response to climate change. *Environmental Geology*, *44*(3), 277–289. https://doi.org/10.1007/s00254-003-0762-9

Bachu, S., Bonijoly, D., Bradshaw, J., Burruss, R., Christensen, N. P., Holloway, S., … Forum, C. S. L. (2007). Phase II Final Report from the Task Force for Review and Identification of Standards for CO2 Storage Capacity Estimation. In *Estimation of CO2 Storage Capacity in Geological Media - Phase 2 -*.

Bachu, S., Shaw, J. C., & Pearson, R. M. (2004). Estimation of oil recovery and CO2 storage capacity in CO2 EOR incorporating the effect of underlying aquifers. *Proceedings - SPE Symposium on Improved Oil Recovery*, *2004-April*, 1–13. https://doi.org/10.2523/89340-ms

Bloomberg. (2022). *"Energy and Oil Prices", www.bloomberg.com/energy, accessed May. 21, 2022*.

Carcoana, A. N. (1982, April 4). Enhanced Oil Recovery in Rumania. *SPE Enhanced Oil Recovery Symposium*, p. SPE-10699-MS. https://doi.org/10.2118/10699-MS

Chadwick, A., Arts, R., Bernstone, C., May, F., Thibeau, S., & Zweigel, P. (2008). *BEST PRACTICE FOR THE STORAGE OF CO 2 IN SALINE AQUIFERS Observations and guidelines from the SACS and CO2STORE projects Derived from projects receiving financial support from the European Union*. Retrieved from http://nora.nerc.ac.uk/id/eprint/2959/1/0812_CO2STORE_BPM_book_V7.pdf

CITA. (2004). *CITA (Companies Income Tax) Act Cap C21, LFN 2004 (as amended)*.

Cremon, M. A., Christie, M. A., & Gerritsen, M. G. (2020a). Monte Carlo simulation for uncertainty quantification in reservoir simulation: A convergence study. *Journal of Petroleum Science and Engineering*. https://doi.org/10.1016/j.petrol.2020.107094

Cremon, M. A., Christie, M. A., & Gerritsen, M. G. (2020b). Monte Carlo simulation for uncertainty quantification in reservoir simulation: A convergence study. *Journal of Petroleum Science and Engineering*, *190*(January), 107094. https://doi.org/10.1016/j.petrol.2020.107094

Cunha, J. C. (2007). *Importance of economie and risk analysis on today's petroleum engineering education*. *2*, 768–772. https://doi.org/10.2523/109638-MS

Dai, Z., Zhang, Y., Stauffer, P., Xiao, T., Zhang, M., Ampomah, W., … Bielicki, J. M. (2017). Injectivity Evaluation for Offshore CO2Sequestration in Marine Sediments. *Energy Procedia*, *114*(November 2016), 2921–2932. https://doi.org/10.1016/j.egypro.2017.03.1420

Doust H., & Omatsola E. M. (1990). Niger Delta. In: Edwards, Santogrossi (eds) Divergent/passive margin basins. *American Association of Petroleum Geologist*, (Mem 48), 201–238.

Echendu, J. C., & Iledare, O. O. (2016). Progressive Royalty Framework for Oil- and Gas-Development Strategy: Lessons From Nigeria. *SPE Economics & Management*, *8*(03), 68–77. https://doi.org/10.2118/174846-PA

Esmaiel, T., Fallah Bolandtaba, S., & van Kruisdijk, cor. (2007). *Determination of WAG Ratios and Slug Sizes Under Uncertainty in a Smart Wells Environment*. https://doi.org/10.2523/93569-ms

ETF. (1993). *ETF (Education Trust Fund) Decree No. 7 of 1993, Federal Government of Nigeria*.

Gaspar Ravagnani, A. T. F. S., Ligero, E. L., & Suslick, S. B. (2009). CO2 sequestration through enhanced oil recovery in a mature oil field. *Journal of Petroleum Science and Engineering*, *65*(3–4), 129–138. https://doi.org/10.1016/J.PETROL.2008.12.015

Ghaderi, S. M., Clarkson, C. R., Taheri, S., & Chen, S. (2013). Investigation of Economic Uncertainties of CO EOR and Sequestration in Tight Oil Formations. *SPE Enhanced Oil Recovery Conference*, (Bachu 2003). https://doi.org/10.2118/165301-MS

Ghomian, Y. (2008). Reservoir Simulation Studies for Coupled CO 2 Sequestration and Committee : *PhD Dissertation*, (Austin, US).

Glasø, Ø. (1985). Generalized Minimum Miscibility Pressure Correlation. *Society of Petroleum Engineers Journal*, *25*(06), 927–934. https://doi.org/10.2118/12893-PA

Godec, M. L., Kuuskraa, V. A., & Dipietro, P. (2013). Opportunities for using anthropogenic CO2 for enhanced oil recovery and CO2 storage. *Energy and Fuels*, *27*(8), 4183–4189. https://doi.org/10.1021/ef302040u

Gozalpour, F., Ren, S. R., & Tohidi, B. (2005). CO2EOR and storage in oil reservoirs. *Oil and Gas Science and Technology*, *60*(3), 537–546. https://doi.org/10.2516/ogst:2005036

He, L., Shen, P., Liao, X., Li, F., Gao, Q., & Wang, Z. (2016). Potential evaluation of CO2 EOR and sequestration in Yanchang oilfield. *Journal of the Energy Institute*, *89*(2), 215–221. https://doi.org/10.1016/j.joei.2015.02.002

Helton, J. C., & Davis, F. J. (2003). Latin hypercube sampling and the propagation of uncertainty in analyses of complex systems. *Reliability Engineering & System Safety*, *81*(1), 23–69. https://doi.org/https://doi.org/10.1016/S0951-8320(03)00058-9

Hill, B., Hovorka, S., & Melzer, S. (2013). Geologic carbon storage through enhanced oil recovery. *Energy Procedia*. https://doi.org/10.1016/j.egypro.2013.06.614

IEAGHG. (2009). *CO2 Storage in Depleted Gas*.

IHS MARKIT. (2016). *CO2 EOR Potential in North Dakota*. (June), 1–101. Retrieved from http://www.legis.nd.gov/files/committees/64-2014 appendices/IHS Energy - Final

Report.pdf

Jia, W., McPherson, B., Pan, F., Dai, Z., & Xiao, T. (2018). Uncertainty quantification of CO2storage using Bayesian model averaging and polynomial chaos expansion. *International Journal of Greenhouse Gas Control*, *71*(June), 104–115. https://doi.org/10.1016/j.ijggc.2018.02.015

Juanes, R., Spiteri, E. J., Orr, F. M., & Blunt, M. J. (2006). Impact of relative permeability hysteresis on geological CO2 storage. *Water Resources Research*, *42*(12), 1–13. https://doi.org/10.1029/2005WR004806

Kamari, A., Arabloo, M., Shokrollahi, A., Gharagheizi, F., & Mohammadi, A. H. (2015). Rapid method to estimate the minimum miscibility pressure (MMP) in live reservoir oil systems during CO2 flooding. *Fuel*, *153*, 310–319. https://doi.org/10.1016/j.fuel.2015.02.087

Kaplan, A., Lusser, C., & Norton, I. (1994). Tectonic Map of the World. *American Association of Petroleum Geologist*, (60), 230–237.

Kehinde, D. O., & Ahzegbobor, P. A. (2015). Hydrocarbon trapping mechanism and petrophysical analysis of Afam field, offshore Nigeria. *International Journal of Physical Sciences*, *10*(7), 222–238. https://doi.org/10.5897/ijps2015.4275

Kemp, A., & Stephen, L. (2015). The economics of EOR schemes in the UK continental shelf (UKCS). *SPE Offshore Europe Conference and Exhibition, OE 2015*, (September), 8–11. Retrieved from https://www.scopus.com/inward/record.uri?eid=2-s2.0-84962359424&partnerID=40&md5=57cc952d0f0aad011ee90042c6d17c77

Klins, M. A. (1984). *CO2 — Heavy Oil Flooding — Economic Design BT - Heavy Crude Oil Recovery* (E. Okandan, Ed.). https://doi.org/10.1007/978-94-009-6140-1_7

Kovscek, A. R. (2002). Screening criteria for CO2storage in oil reservoirs. *Petroleum Science and Technology*, *20*(7–8), 841–866. https://doi.org/10.1081/LFT-120003717

Kulke, H. [ed. . (1995). *Regional petroleum geology of the world. Pt. 2. Africa, America, Australia and Antarctica*. https://doi.org/https://doi.org/

Kumar, S., & Mandal, A. (2017). A comprehensive review on chemically enhanced water alternating gas/CO2(CEWAG) injection for enhanced oil recovery. *Journal of Petroleum Science and Engineering*, *157*(July), 696–715. https://doi.org/10.1016/j.petrol.2017.07.066

Land, C. S. (1968). Calculation of Imbibition Relative Permeability for Two- and Three-Phase Flow From Rock Properties. *Society of Petroleum Engineers Journal*, *8*(02), 149–156. https://doi.org/10.2118/1942-PA

Larsen A., J. A. . S. (1995). Comparing Hysteresis Models for Relative Permeability in WAG Studies. *Sca*, (9506).

Lashkarbolooki, M., Eftekhari, M. J., Najimi, S., & Ayatollahi, S. (2017). Minimum miscibility pressure of CO2and crude oil during CO2injection in the reservoir. *Journal of Supercritical Fluids*, *127*(April), 121–128. https://doi.org/10.1016/j.supflu.2017.04.005

Lawal, Kazeem A. (2011, July 30). An Improved Estimation of the Storage Capacity of Potential Geologic Carbon-Sequestration Sites. *Nigeria Annual International Conference and Exhibition*, p. SPE-150739-MS. https://doi.org/10.2118/150739-MS

Lawal, Kazeem Akintayo. (2011). *Alternating Injection of Steam and CO_2 For Thermal Recovery of Heavy Oil*. (August), 327.

Leung, D. Y. C., Caramanna, G., & Maroto-Valer, M. M. (2014). An overview of current status of carbon dioxide capture and storage technologies. *Renewable and Sustainable Energy Reviews*, *39*, 426–443. https://doi.org/10.1016/j.rser.2014.07.093

Li, H., & Durlofsky, L. J. (2016). Local–Global Upscaling for Compositional Subsurface Flow Simulation. *Transport in Porous Media*, *111*(3), 701–730. https://doi.org/10.1007/s11242-015-0621-7

Liang, Z., Shu, W., Li, Z., Shaoran, R., & Qing, G. (2009). Assessment of CO2EOR and its geo-storage potential in mature oil reservoirs, Shengli Oilfield, China. *Petroleum Exploration and Development*, *36*(6), 737–742. https://doi.org/10.1016/S1876-3804(10)60006-7

Liu, L., Zhang, T., Zhao, X., Wu, S., Hu, J., Wang, X., & Zhang, Y. (2013a). Sedimentary architecture models of deepwater turbidite channel systems in the Niger Delta continental slope, West Africa. *Petroleum Science*, *10*(2), 139–148. https://doi.org/10.1007/s12182-013-0261-x

Liu, L., Zhang, T., Zhao, X., Wu, S., Hu, J., Wang, X., & Zhang, Y. (2013b). Sedimentary architecture models of deepwater turbidite channel systems in the Niger Delta continental slope, West Africa. *Petroleum Science*, *10*(2), 139–148. https://doi.org/10.1007/s12182-013-0261-x

Luna, A. (2013). *3D Seismic Analysis and Characterization of a Stacked Turbidite Channel : Niger Delta Complex*.

Martin, D. F., & Taber, J. J. (1992). Carbon Dioxide Flooding. *Journal of Petroleum Technology*, *44*(04), 396–400. https://doi.org/10.2118/23564-PA

McCoy, S. T., & Rubin, E. S. (2008). An engineering-economic model of pipeline transport

of CO2 with application to carbon capture and storage. *International Journal of Greenhouse Gas Control*, *2*(2), 219–229. https://doi.org/https://doi.org/10.1016/S1750-5836(07)00119-3

Mokhtari, R., Ayatollahi, S., Hamid, K., & Zonnouri, A. (2016). Co-optimization of Enhanced Oil Recovery and Carbon Dioxide Sequestration in a Compositionally Grading Iranian Oil Reservoir; Technical and Economic Approach. *Abu Dhabi International Petroleum Exhibition & Conference*. https://doi.org/10.2118/183560-MS

Montgomery, D. C. (2008). *Design and Analysis of Experiments*.

Naderi, S., & Simjoo, M. (2019). Numerical study of Low Salinity Water Alternating CO 2 injection for enhancing oil recovery in a sandstone reservoir: Coupled geochemical and fluid flow modeling. *Journal of Petroleum Science and Engineering*, *173*(October 2018), 279–286. https://doi.org/10.1016/j.petrol.2018.10.009

Namdie, I., Akpabio, I., & Okechukwu .E., A. (2017). Shale volume and permeability of the Miocene unconsolidated turbidite sands of Bonga oil field, Niger delta, Nigeria. *International Journal of Advanced Geosciences*, *5*(1), 37. https://doi.org/10.14419/ijag.v5i1.7586

National Energy Board of Canada (NEB). (2006). *Canada's Oil Sands, Opportunities & Challenges to 2015: An Update*. Calgary.

Neal, P. R., Hou, W., Allinson, W. G., & Cinar, Y. (2010, October 18). Costs of CO2 Transport and Injection in Australia. *SPE Asia Pacific Oil and Gas Conference and Exhibition*, p. SPE-133900-MS. https://doi.org/10.2118/133900-MS

Nigerian Investment Promotion Commission (NIPC). (2010, December 19). *Investors' Guide to Nigeria, 5th ed.,*. Retrieved from www.cbcglobal.org/CBCG_Library

Nogueira, M. C., & Mamora, D. D. (2005, March 7). Effect of Flue Gas Impurities on the Process of Injection and Storage of CO2 in Depleted Gas Reservoirs. *SPE/EPA/DOE Exploration and Production Environmental Conference*, p. SPE-94906-STU. https://doi.org/10.2118/94906-STU

Ofurhie, M. A., Lufadeju, A. O., Agha, G. U., & Ineh, G. C. (2008). *Turbidite Depositional Environment In Deepwater Of Nigeria*. https://doi.org/10.4043/14068-ms

Ogbeiwi, P, Stephen, K., & Akinroola, A. (2020). *Optimisation of Waterflooding under Geological Uncertainties Using an Adaptive Data-Driven Surrogate: Case Study*. *2020*(1), 1–5. https://doi.org/https://doi.org/10.3997/2214-4609.202011968

Ogbeiwi, P, Stephen, K., & Arinkoola, A. (2020). *A Surrogate-Based Approach to Waterflood Optimisation under Uncertainty*. *2020*(1), 1–16.

https://doi.org/https://doi.org/10.3997/2214-4609.202035076

Ogbeiwi, Precious, Stephen, K. D., & Arinkoola, A. O. (2020). Robust optimisation of water flooding using an experimental design-based surrogate model: A case study of a Niger-Delta oil reservoir. *Journal of Petroleum Science and Engineering*, *195*(September), 107824. https://doi.org/10.1016/j.petrol.2020.107824

Oni, S. I., & Oyewo, M. A. (2011). Gas Flaring, Transportation and Sustainable Energy Development in the Niger-Delta, Nigeria. *Journal of Human Ecology*, *33*(1), 21–28. https://doi.org/10.1080/09709274.2011.11906345

Onwuka, E. I., Iledare, O. O., & Echendu, J. C. (2012, August 6). Evaluating the Impact of Depreciation Methods and Production Decline Patterns on Deepwater Economics: A Case Study of Nigeria. *Nigeria Annual International Conference and Exhibition*, p. SPE-163007-MS. https://doi.org/10.2118/163007-MS

Opara, A. I. (2011). Estimation of multiple sources of overpressures using vertical effective stress approach: Case study of the Niger Delta, Nigeria. *Petroleum and Coal*, *53*(4), 302–314.

Oyeyemi, K. D., Olowokere, M. T., & Aizebeokhai, A. P. (2018). Hydrocarbon resource evaluation using combined petrophysical analysis and seismically derived reservoir characterization, offshore Niger Delta. *Journal of Petroleum Exploration and Production Technology*, *8*(1), 99–115. https://doi.org/10.1007/s13202-017-0391-6

Pham, V., & Halland, E. (2017). Perspective of CO2for Storage and Enhanced Oil Recovery (EOR) in Norwegian North Sea. *Energy Procedia*, *114*(November 2016), 7042–7046. https://doi.org/10.1016/j.egypro.2017.03.1845

PIB. (2009). *PIB (Petroleum Industry Bill) of 2009 (as amended*.

PPT. (1990). *PPT (Petroleum Profits Tax) Act Cap 354 Laws of the Federation of Nigeria (LFN) 1990*.

PTDF. (1990). *PTDF (Petroleum Technology Development Fund) Act Cap.355 Laws of the Federation of Nigeria (LFN) 1990*.

Ramírez, A., Hagedoorn, S., Kramers, L., Wildenborg, T., & Hendriks, C. (2010). Screening CO2 storage options in The Netherlands. *International Journal of Greenhouse Gas Control*, *4*(2), 367–380. https://doi.org/10.1016/j.ijggc.2009.10.015

Raza, A., Rezaee, R., Gholami, R., Bing, C. H., Nagarajan, R., & Hamid, M. A. (2016). A screening criterion for selection of suitable CO2storage sites. *Journal of Natural Gas Science and Engineering*, *28*, 317–327. https://doi.org/10.1016/j.jngse.2015.11.053

Rhodes, C. J. (2013). Current Commentary; Carbon capture and storage. *Science Progress*,

95(4), 473–483. https://doi.org/10.3184/003685012x13505722145181

Safi, R., Agarwal, R. K., & Banerjee, S. (2016). Numerical simulation and optimization of CO2utilization for enhanced oil recovery from depleted reservoirs. *Chemical Engineering Science*, *144*, 30–38. https://doi.org/10.1016/j.ces.2016.01.021

Shahverdi, H., & Sohrabi, M. (2015). Modeling of cyclic hysteresis of three-phase relative permeability during water-alternating-gas injection. *SPE Journal*, *20*(1), 35–48. https://doi.org/10.2118/166526-pa

Shell. (2001). EP00- Introducing the E & P Business. In *Shell Learning Centre, The Netherlands*.

Solomon, S. (2006). *Criteria for Intermediate Storage of Carbon Dioxide in Geological Formations*. (1), 11.

Spiteri, E. J., & Juanes, R. (2006). Impact of relative permeability hysteresis on the numerical simulation of WAG injection. *Journal of Petroleum Science and Engineering*, *50*(2), 115–139. https://doi.org/10.1016/j.petrol.2005.09.004

Spiteri, E., Juanes, R., Blunt, M. J., & Orr, F. M. (2005). Relative-Permeability Hysteresis: Trapping Models and Application to Geological CO2 Sequestration. *SPE Annual Technical Conference and Exhibition*. https://doi.org/10.2118/96448-MS

Stacher, P. (1995). *Present understanding of the Niger Delta hydrocarbon habitat, in, Oti, M.N., and Postma, G., eds., Geology of Deltas: Rotterdam, A.A. Balkema*.

Stevens, S., Kuuskraa, V., & Taber, J. (1999). Sequestration of CO2 in depleted oil and gas fields: Barriers to overcome in implementation of CO2 capture and storage (disused oil and gas fields). *Report for the IEA Greenhouse Gas Research and Development Programme (PH3/22)*, *87*(81A-81).

Stewart, R. J., Johnson, G., Heinemann, N., Wilkinson, M., & Haszeldine, R. S. (2018). Low carbon oil production: Enhanced oil recovery with CO2 from North Sea residual oil zones. *International Journal of Greenhouse Gas Control*. https://doi.org/10.1016/j.ijggc.2018.06.009

Sun, L., & Chen, W. (2022). Impact of carbon tax on CCUS source-sink matching: Finding from the improved ChinaCCS DSS. *Journal of Cleaner Production*, *333*(November 2021), 130027. https://doi.org/10.1016/j.jclepro.2021.130027

Taber, J. J. (1983, October 5). Technical Screening Guides for the Enhanced Recovery of Oil. *SPE Annual Technical Conference and Exhibition*, p. SPE-12069-MS. https://doi.org/10.2118/12069-MS

Tang, Y., Yang, R., & Bian, X. (2014). A review of CO2sequestration projects and

application in China. *Scientific World Journal*, *2014*. https://doi.org/10.1155/2014/381854

Tayari, F., Blumsack, S., Dilmore, R., & Mohaghegh, S. D. (2015). Techno-economic assessment of industrial CO<inf>2</inf> storage in depleted shale gas reservoirs. *Journal of Unconventional Oil and Gas Resources*, *11*, 82–94. https://doi.org/10.1016/j.juogr.2015.05.001

Tuttle, M. L. W., Charpentier, R. R., & Brownfield, M. E. (1999). The Niger Delta Petroleum System: Niger Delta Province, Nigeria, Cameroon, and Equatorial Guinea, Africa. *World Energy Project*, (99-50-H), 64.

Umar, B. A., Gholami, R., Nayak, P., Shah, A. A., & Adamu, H. (2020). Regional and field assessments of potentials for geological storage of CO2: A case study of the Niger Delta Basin, Nigeria. *Journal of Natural Gas Science and Engineering*, *77*(October 2019), 103195. https://doi.org/10.1016/j.jngse.2020.103195

Vahidi, A., Ahmadi, M., & Nourmohammad, A. (2014). Carbon Dioxide Minimum Miscibility Pressure Estimation (Case Study). *Journal of Petroleum Science and Technology*, *4*(2), 20–27.

Van Der Meer, B. (2005). Carbon Dioxide Storage in Natural Gas Reservoir. *Oil \& Gas Science and Technology - Rev. IFP*, *60*(3), 527–536. https://doi.org/10.2516/ogst:2005035

Vulin, D., Gaćina, M., & Biličić, V. (2018). Slim-Tube Simulation Model for Co2 Injection Eor. *Rudarsko-Geološko-Naftni Zbornik*, *33*(2), 37–48. https://doi.org/10.17794/rgn.2018.2.4

Wang, X., van ’t Veld, K., Marcy, P., Huzurbazar, S., & Alvarado, V. (2018). Economic co-optimization of oil recovery and CO2 sequestration. *Applied Energy*, *222*(April), 132–147. https://doi.org/10.1016/j.apenergy.2018.03.166

Weber, K. J., & Daukoru, E. M. (1975). Petroleum Geology of the Niger Delta. *Proceeding of the Ninth World Petroleum Congress, Tokyo*, *2*, 209–221.

Wei, N., Li, X., Dahowski, R. T., Davidson, C. L., Liu, S., & Zha, Y. (2015a). Economic evaluation on CO2-EOR of onshore oil fields in China. *International Journal of Greenhouse Gas Control*, *37*, 170–181. https://doi.org/10.1016/j.ijggc.2015.01.014

Wei, N., Li, X., Dahowski, R. T., Davidson, C. L., Liu, S., & Zha, Y. (2015b). Economic evaluation on CO2-EOR of onshore oil fields in China. *International Journal of Greenhouse Gas Control*, *37*, 170–181. https://doi.org/10.1016/j.ijggc.2015.01.014

Welkenhuysen, K., Meyvis, B., & Piessens, K. (2017). A Profitability Study of CO2-EOR

and Subsequent CO2Storage in the North Sea under Low Oil Market Prices. *Energy Procedia*, *114*(November 2016), 7060–7069. https://doi.org/10.1016/j.egypro.2017.03.1848

Welkenhuysen, K., Rupert, J., Compernolle, T., Ramirez, A., Swennen, R., & Piessens, K. (2017). Considering economic and geological uncertainty in the simulation of realistic investment decisions for CO2-EOR projects in the North Sea. *Applied Energy*, *185*, 745–761. https://doi.org/10.1016/j.apenergy.2016.10.105

Yang, C., Card, C., & Nghiem, L. (2007, June 12). Economic Optimization and Uncertainty Assessment of Commercial SAGD Operations. *Canadian International Petroleum Conference*, p. PETSOC-2007-029. https://doi.org/10.2118/2007-029

Zhao, F. (2001). *The principle of EOR*. Petroleum University Press, Chengdu.

Graphical Abstract

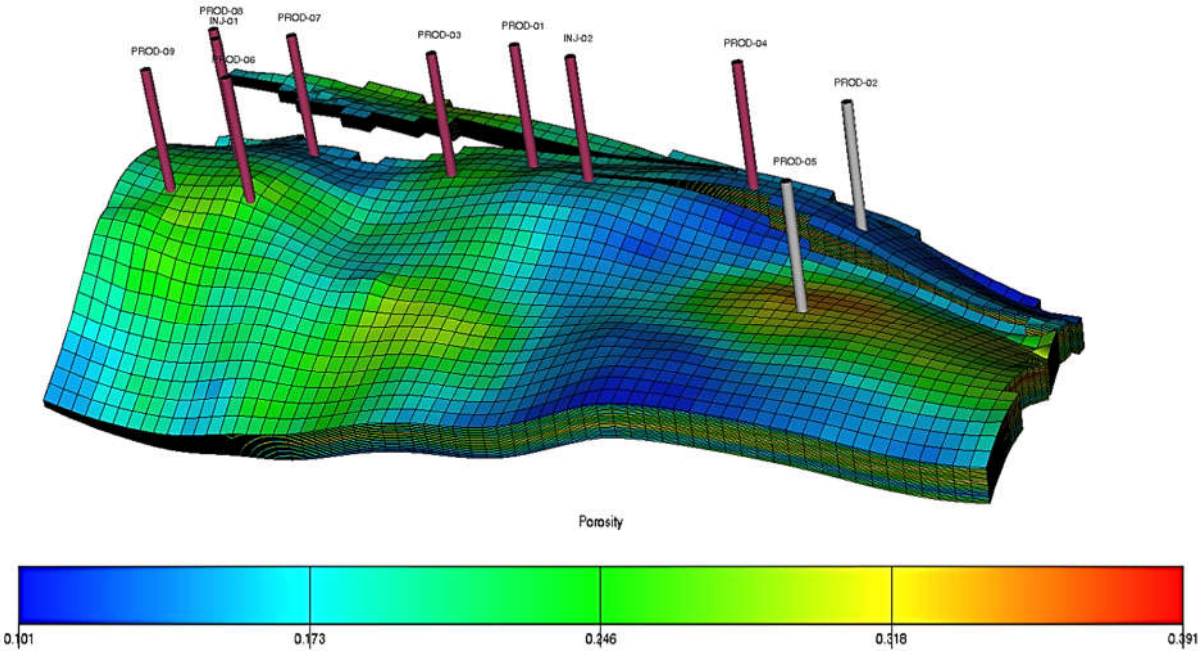

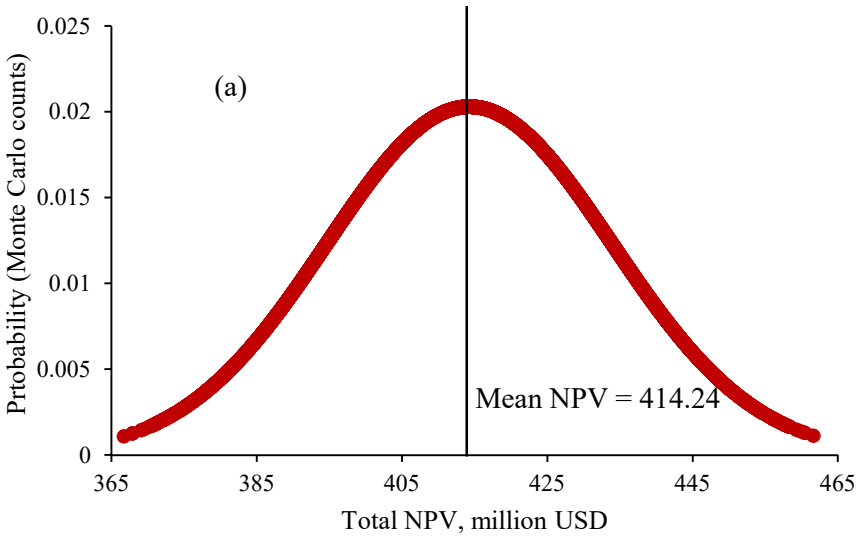
(a)
Prtobability (Monte Carlo counts)
0.025
0.02
0.015
0.01
0.005
0
Mean NPV = 414.24
365
385
405
425
445
465
Total NPV, million USD